# Current Status of the Muon g-2 Experiment at Fermilab

Tammy Walton

Aspen 2018 : The Particle Frontier

March 27, 2018

# Outline

- Muon g-2 Physics
- Muon g-2 Experiment
- Muon g-2 Status
- Conclusions

$\vec{\mu}$ = magnetic moment
$\vec{S}$ = spin
g = g-factor
q = charge
m = mass

$$\vec{\mu} = g \frac{q}{2m} \vec{S}$$

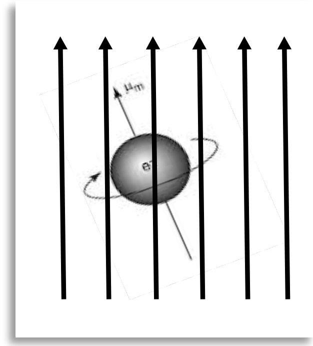

$g =$

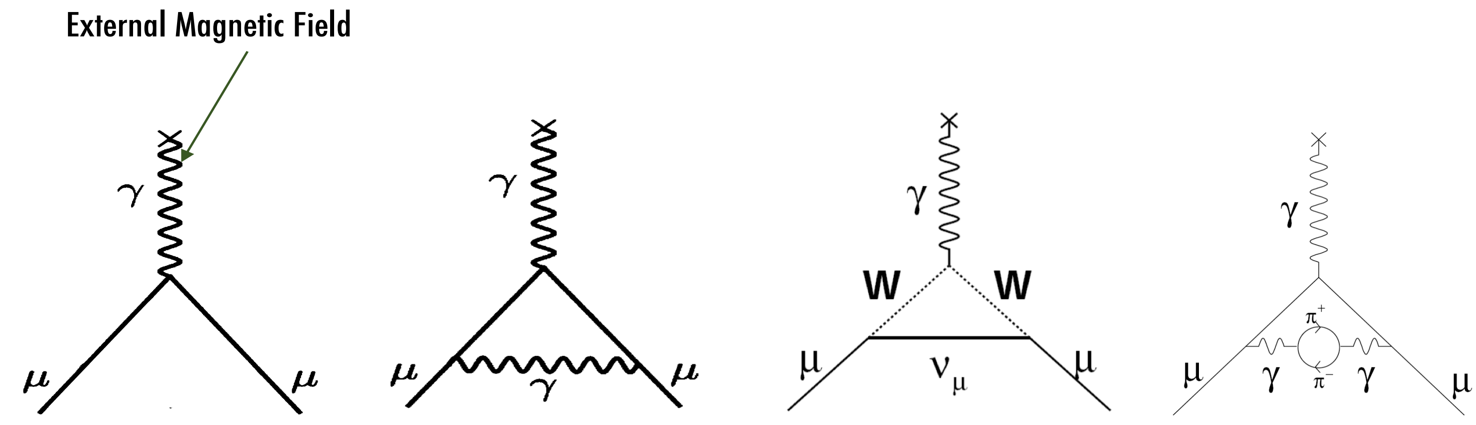


$$g = 2(1 + a)$$

$$a_\mu^{SM} = {(g-2)}/{2} = a^{QED} + a^{EW} + a^{QCD}$$

muon anomalous magnetic moment

$$a_\mu^{SM} = {(g-2)}/{2} = a^{QED} + a^{EW} + a^{QCD}$$

$$\left.\begin{aligned} a_\mu^{QED} &= 0.00116584718951 \\ a_\mu^{EW} &= 0.00000000154 \\ a_\mu^{QCD} &= 0.00000006930 \end{aligned}\right\} a_\mu^{SM} = 0.00\,116\,591\,802\,(49)$$

$$a_\mu^{EX} = 0.00\,116\,592\,089\,(63)$$

$$\boxed{a_\mu^{EXP} - a_\mu^{SM} = 0.00000000287\,(80) > 3\sigma}$$

$$\Downarrow$$

$$\boxed{a_\mu^{EXP} - a_\mu^{SM} = a_\mu^{New\ Physics}}$$

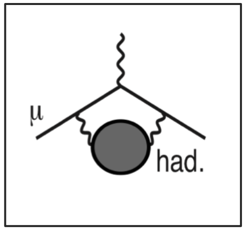


$$a_\mu^{SM} = {(g-2)}/{2} = a^{QED} + a^{EW} + a^{QCD}$$

Place to reduce the uncertainty

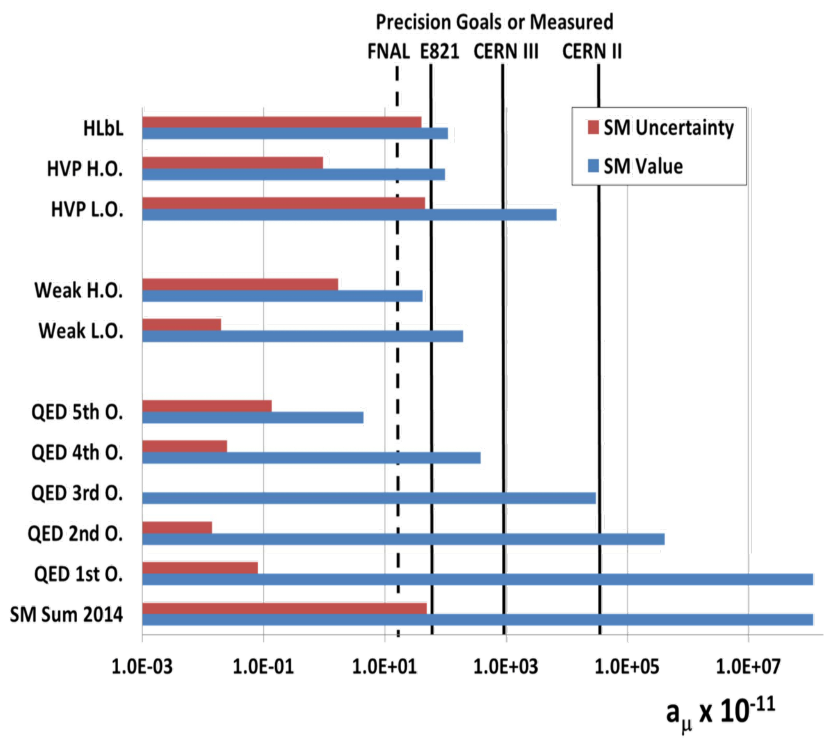


https://arxiv.org/pdf/1710.06874.pdf

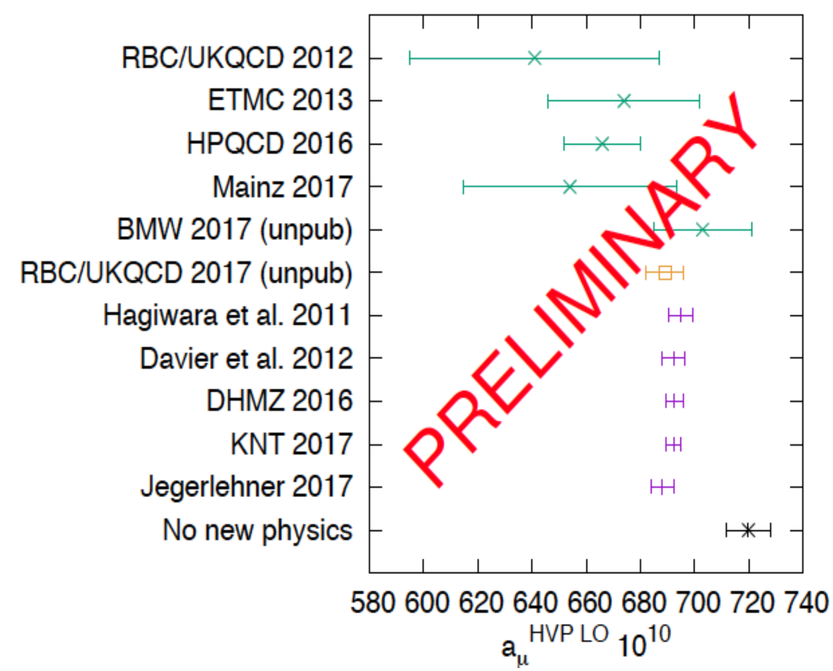


From talk by C. Lehner at Lattice 2017

Lattice Calculation — Both

Dispersion Relation Based on data from $e^+e^- \to$ hadrons

Theory talk by Aida El-Khadra, "The Muon g-2 Theory Initiative" on March 26, 2018

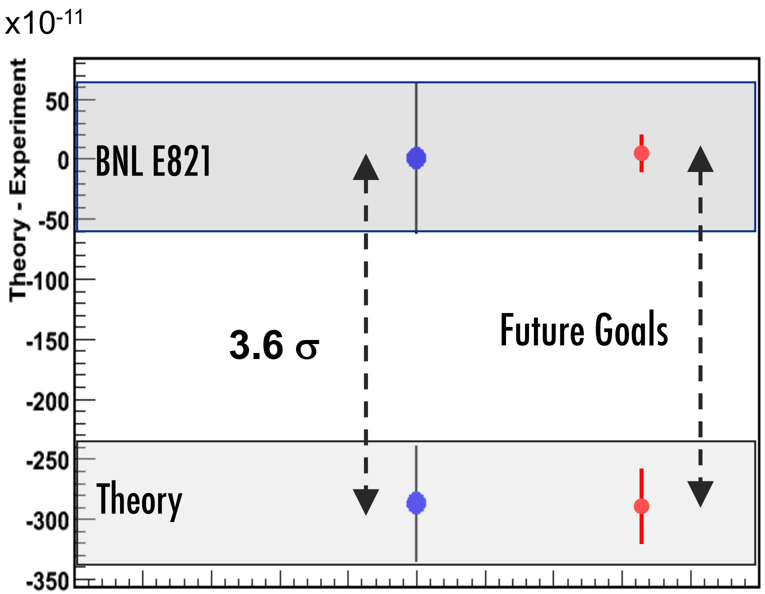


> 7 σ for unchanged central values

New Physics!

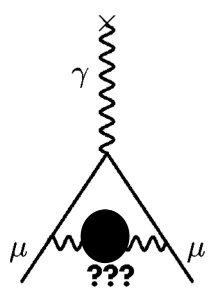


| Uncertainty Source $\delta a_\mu$ | Status 2015 [ppb] | Projected after FNAL [ppb] |
|---|---|---|
| Total Theory | 420 | 310 |
| HVP | 360 | 215 |
| HLbL | 225 | 225 |
| Total Exp. | 540 | 140 |

Theory uncertainty remains the same, both the theoretical and experimental central values are unchanged, but the experimental uncertainty is reduced.

5 σ discrepancy

# Outline

- Muon g-2 Physics
- Muon g-2 Experiment
- Muon g-2 Status
- Conclusions

Brookhaven Muon g-2 Experiment


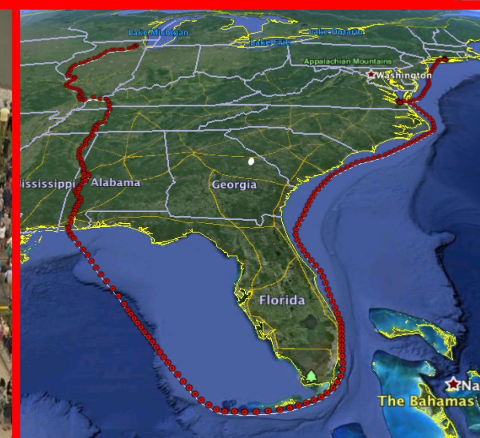


BNL experiment was statistically limited.

Need more muons!

Lets move to Fermilab!

Reduce the 480 ppb statistical uncertainty to 100 ppb! → 10 x BNL data

# Technical Design Report

Table 5.1: Event rate calculation using a bottom-up approach.

| Item | Factor | Value per fill | Note |
|---|---|---|---|
| Protons on target | | $10^{12}$ p | 1 |
| Positive pions captured in FODO, $\delta p/p = \pm 0.5\%$ | $1.2 \times 10^{-4}$ | $1.2 \times 10^{8}$ | 2 |
| Muons captured and transmitted to SR, $\delta p/p = \pm 2\%$ | 0.67% | $8.1 \times 10^{5}$ | 3 |
| Transmission efficiency after commissioning | 90% | $7.3 \times 10^{5}$ | 4 |
| Transmission and capture in SR | $(2.5 \pm 0.5)\%$ | $1.8 \times 10^{4}$ | 5 |
| Stored muons after scraping | 87% | $1.6 \times 10^{4}$ | 6 |
| Stored muons after 30 $\mu s$ | 63% | $1.0 \times 10^{4}$ | 7 |
| Accepted positrons above E = 1.86 GeV | 10.7% | $1.1 \times 10^{3}$ | 8 |
| Fills to acquire $1.6 \times 10^{11}$ events (100 ppb) | | $1.5 \times 10^{8}$ | 9 |
| Days of good data accumulation | 17 h/d | 202 d | 10 |
| Beam-on commissioning days | | 150 d | 11 |
| Dedicated systematic studies days | | 50 d | 12 |
| Approximate running time | | $402 \pm 80$ d | 13 |
| Approximate total proton on target request | | $(3.0 \pm 0.6) \times 10^{20}$ | 14 |

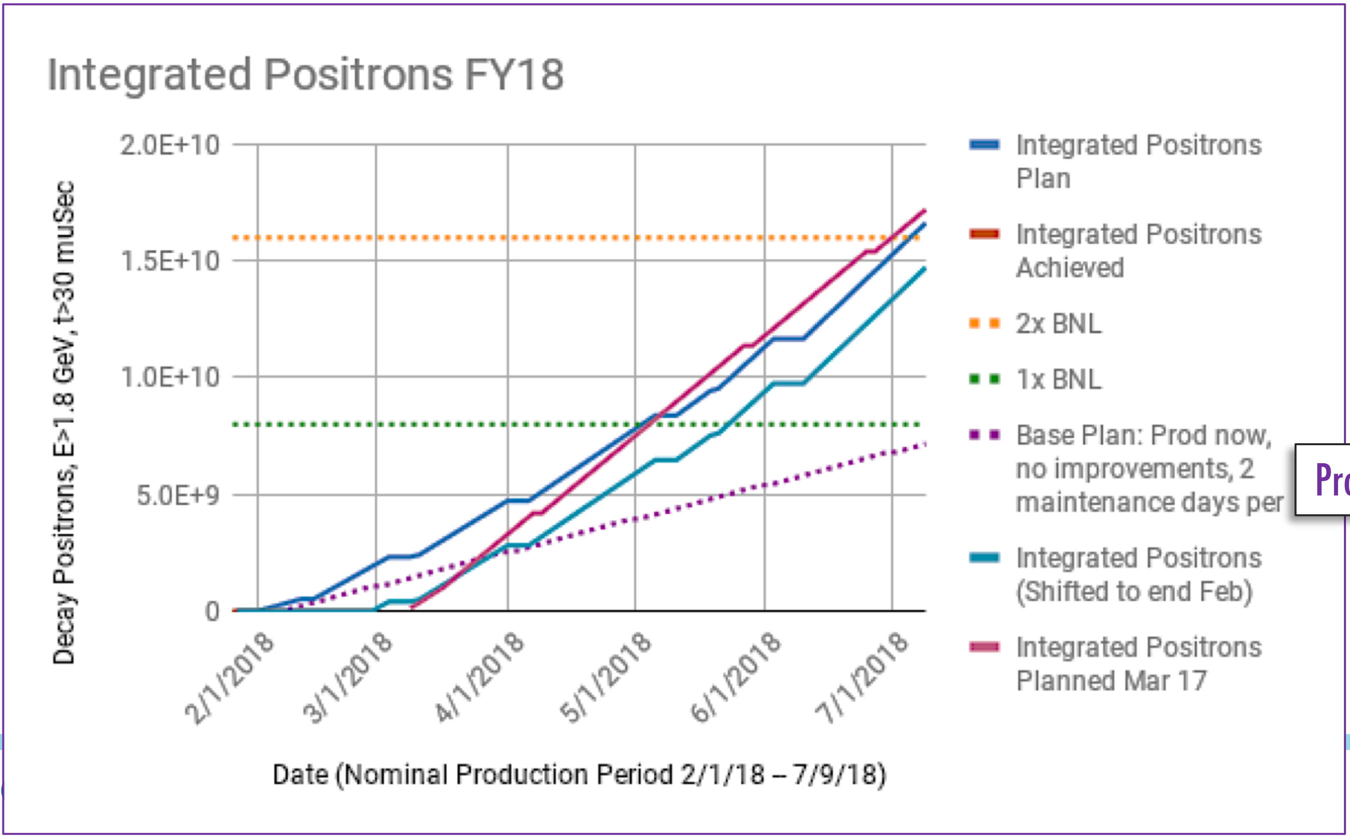


Production uptime 75%


Fermilab

# Fundamental Principles of Measuring Muon g-2

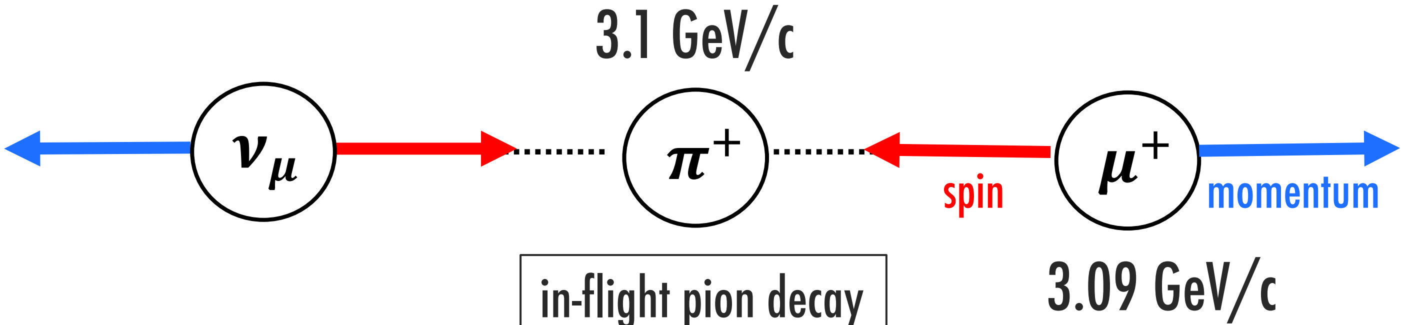


select the highest energy (forward moving) muons

97% polarization

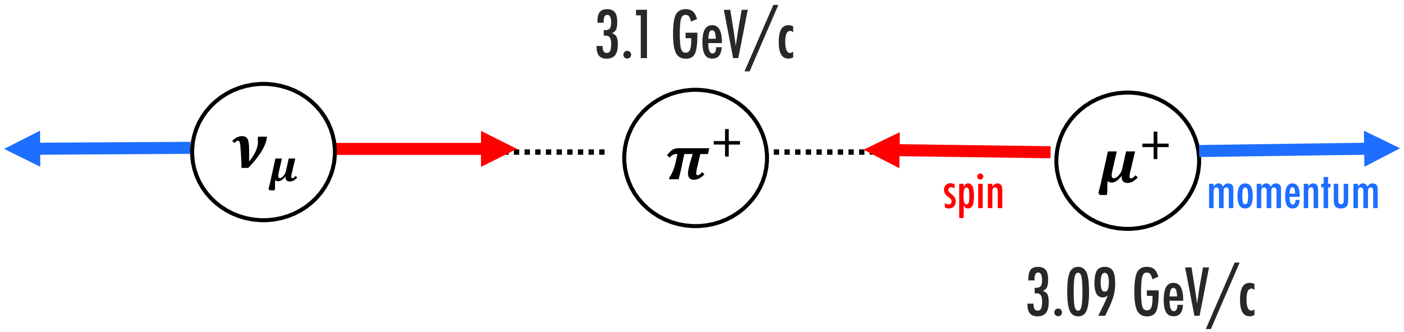


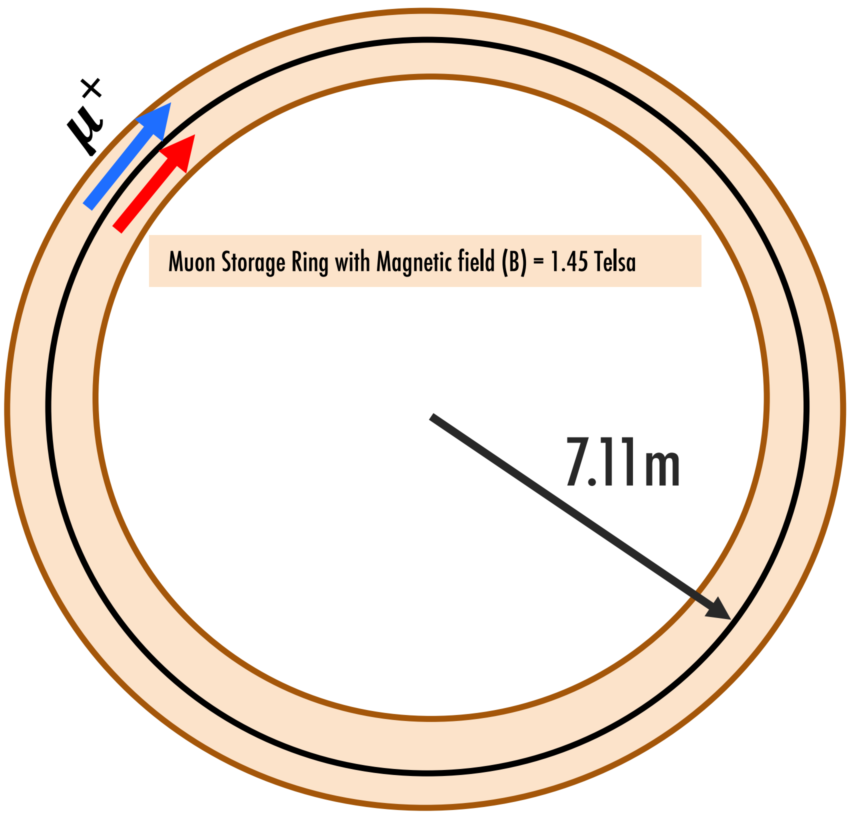


Cyclotron frequency (momentum rotates) $\omega_c = \dfrac{qB}{m_\mu c\gamma}$

Spin precession frequency (spin rotates) $\omega_s = \dfrac{g_\mu qB}{2m_\mu c} + (1-\gamma)\dfrac{qB}{m_\mu c\gamma}$

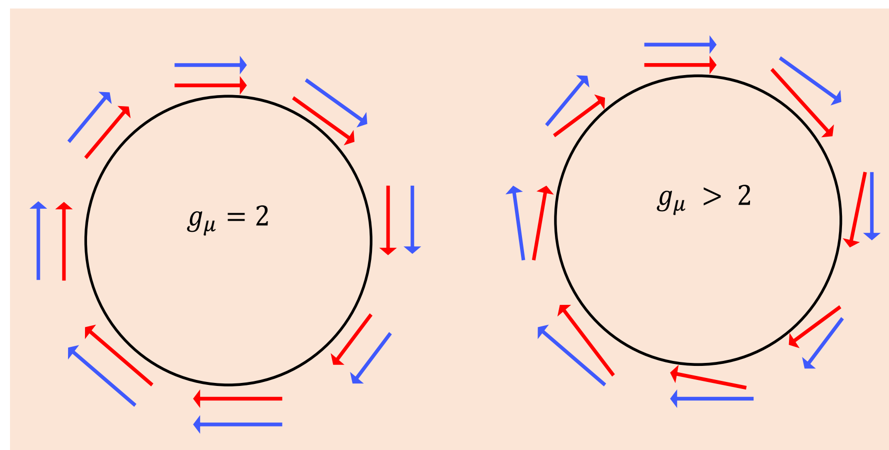


**Precession Rate for g = 2**
Spin and momentum are rotating at the same rate.

**Precession Rate for g > 2**
Spin is rotating faster than the momentum.

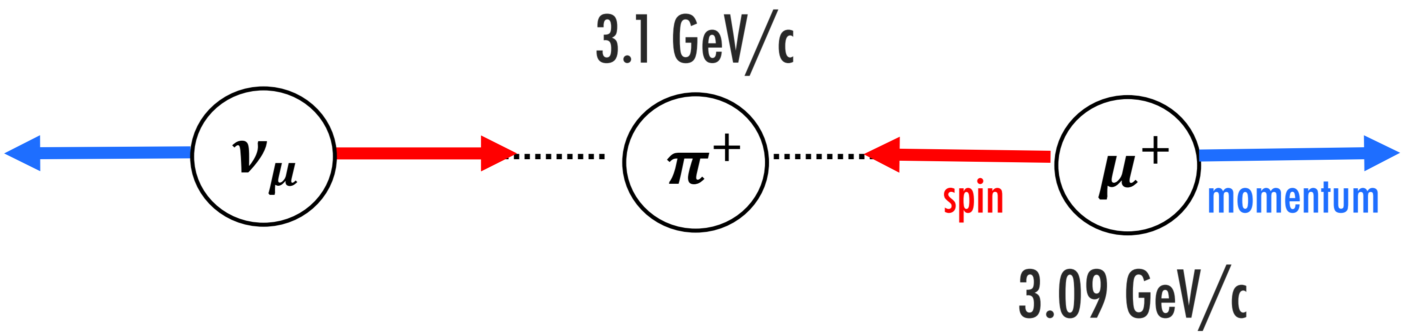


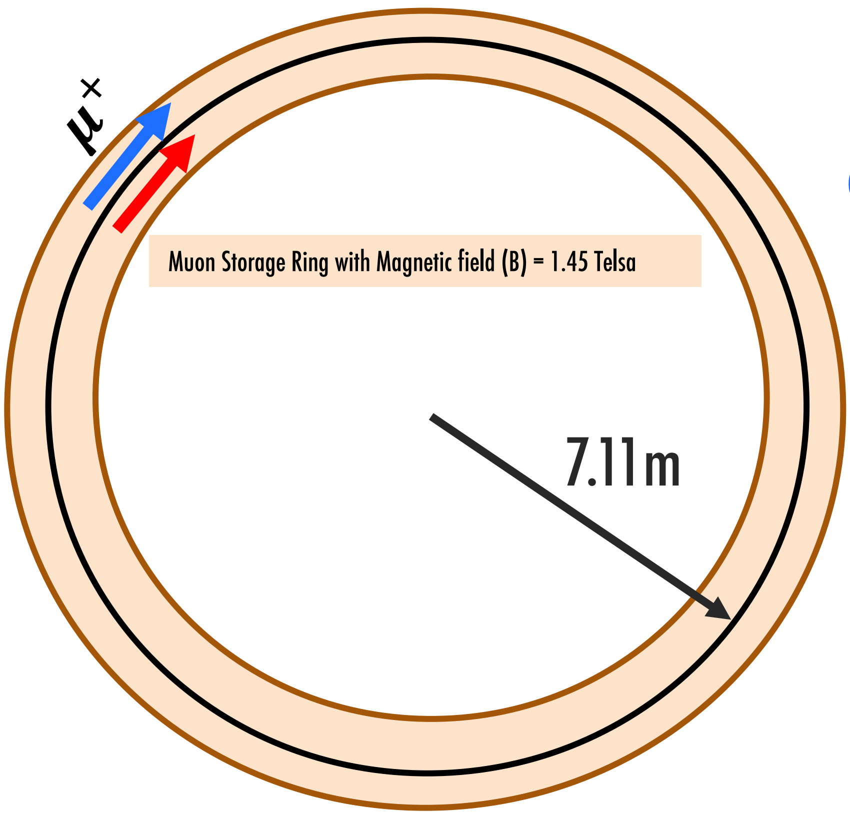


Cyclotron frequency (momentum rotates) $\omega_c = \dfrac{qB}{m_\mu c\gamma}$

Spin precession frequency (spin rotates) $\omega_s = \dfrac{g_\mu qB}{2m_\mu c} + (1-\gamma)\dfrac{qB}{m_\mu c\gamma}$

The difference between the frequencies gives the precession rate.

$$\omega_a = \omega_s - \omega_c = \frac{g_\mu - 2}{2}\frac{qB}{m_\mu c} = a_\mu \frac{qB}{m_\mu c}$$

measurements needed to extract muon g-2


Fermilab

$$\omega_a = a_\mu \frac{qB}{m_\mu c}$$

$$a_\mu(\text{Expt}) = \frac{g_e}{2} \frac{\omega_a}{\tilde{\omega}_p} \frac{m_\mu}{m_e} \frac{\mu_p}{\mu_e}$$

-.001519270384(12) [8 ppb]

206.768 2843(52) [25 ppb]

-2.002 319 304 361 53(53) [0.26 ppt]
Electron g-2 + QED

$\omega_a$ is measured from the muons and $\tilde{\omega}_p$ is measured from the magnetic field.

# Outline

- Muon g-2 Physics
- Muon g-2 Experiment
- Muon g-2 Status
- Conclusions

Magnetic Field = 1.4513 T
Current = 5176 A
3 x 15 m
700 tons
12 Yokes: C shaped flux

$$a_\mu(\text{Expt}) = \frac{g_e}{2}\frac{\omega_a}{\tilde{\omega}_p}\frac{m_\mu}{m_e}\frac{\mu_p}{\mu_e}$$

Detectors

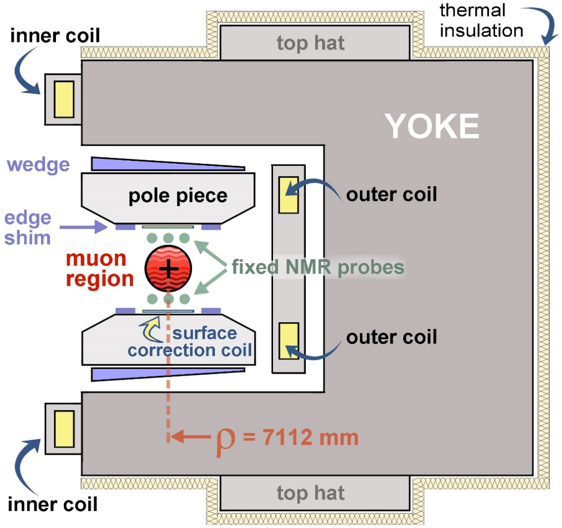


g-2 Magnet in Cross Section

## Results of Shimming the Magnet

FNAL
BNL

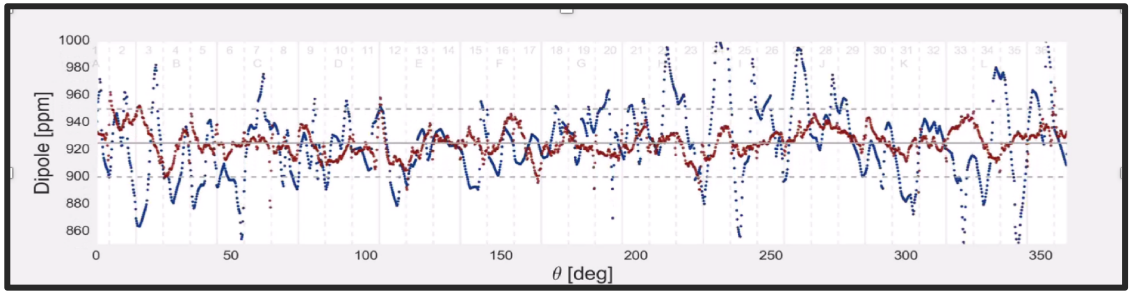


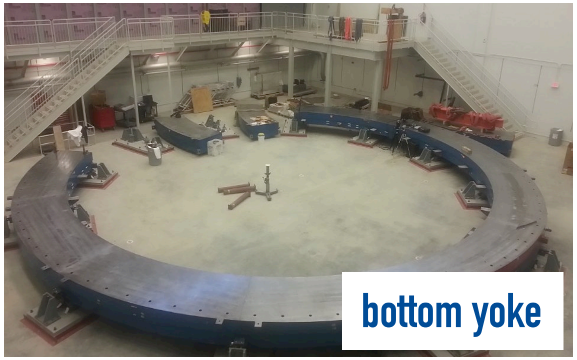

bottom yoke

three superconducting NbTi/Cu coils

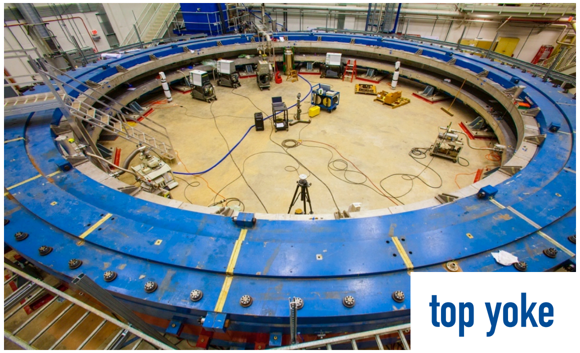

top yoke

$$a_\mu(\mathrm{Expt}) = \frac{g_e}{2}\frac{\omega_a}{\tilde{\omega}_p}\frac{m_\mu}{m_e}\frac{\mu_p}{\mu_e}$$

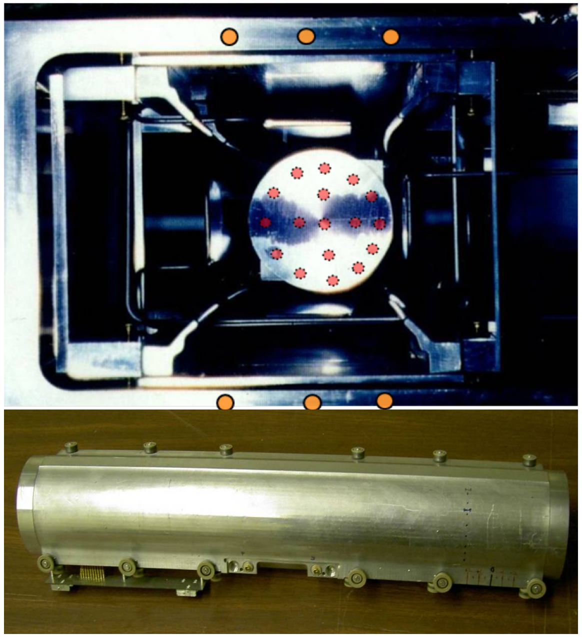

When there is no beam, a trolley pulls 17 proton NMR probes azimuthal over the storage ring .

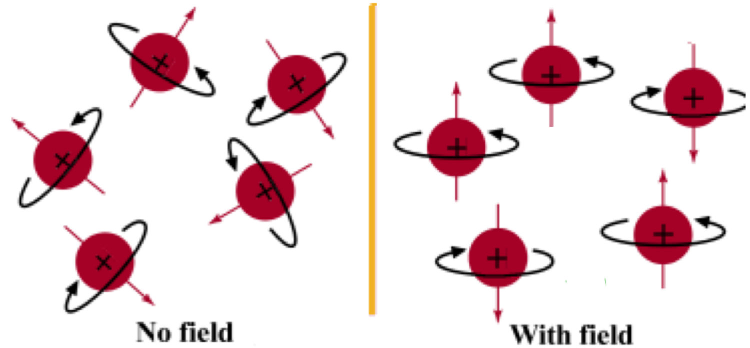


protons precess at a rate proportional to the vertical magnetic field

**Total Systematic Uncertainty**

BNL to FNAL

170 ppb to 70 ppb

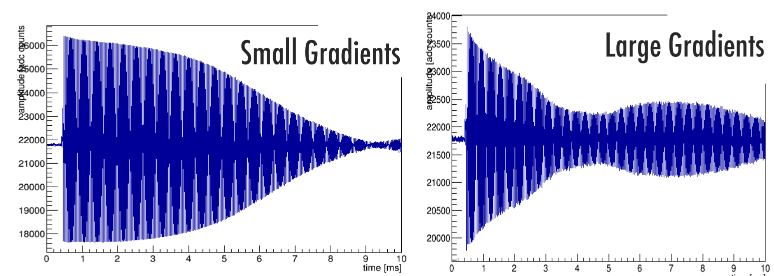


The shape of the free induction decay (FID) provides information about the size of the magnetic field gradients.

Digitizes the waveforms, calibrates, and reconstructs the average magnetic field.

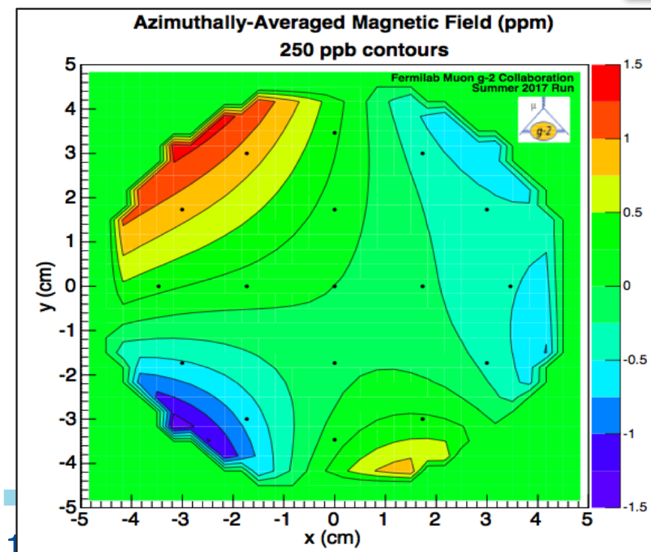


Fermilab

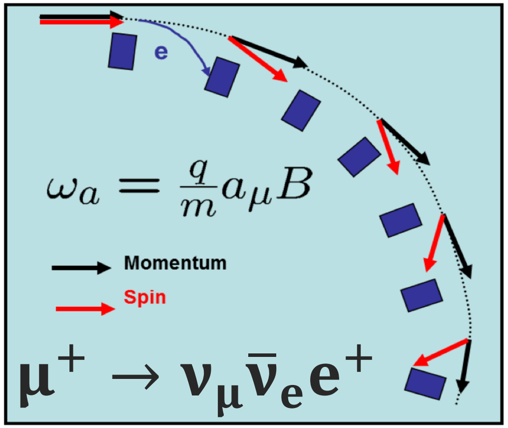


$$a_\mu(\text{Expt}) = \frac{g_e}{2} \frac{\omega_a}{\tilde{\omega}_p} \frac{m_\mu}{m_e} \frac{\mu_p}{\mu_e}$$

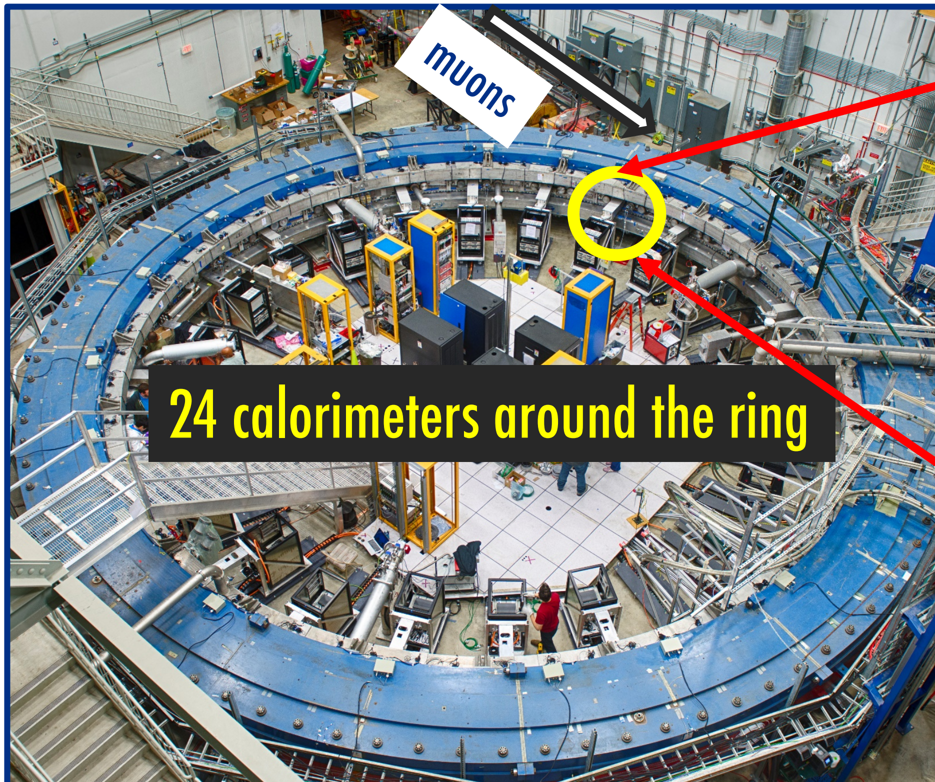


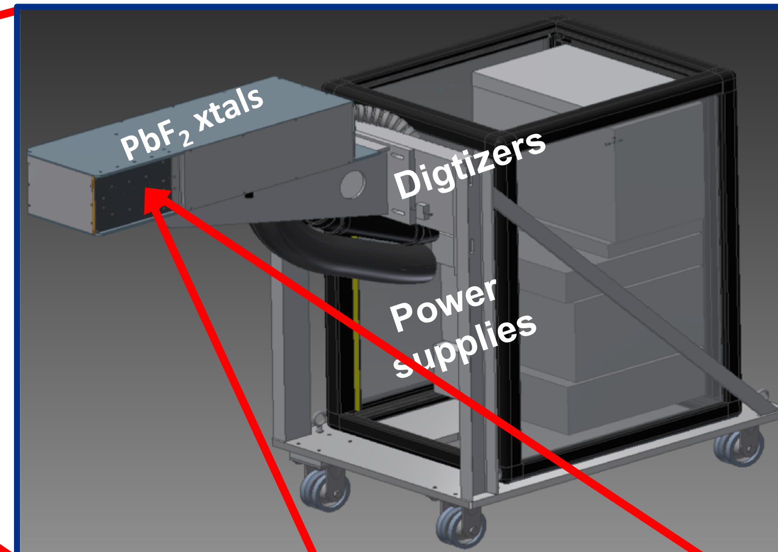


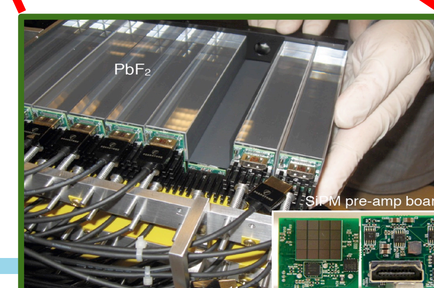

$$\mu^+ \rightarrow \nu_\mu \bar{\nu}_e e^+$$

$$a_\mu(\text{Expt}) = \frac{g_e}{2} \frac{\omega_a}{\tilde{\omega}_p} \frac{m_\mu}{m_e} \frac{\mu_p}{\mu_e}$$

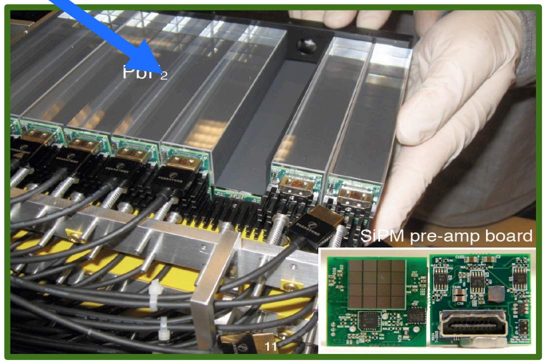


Decay positron showers into the calorimeters.

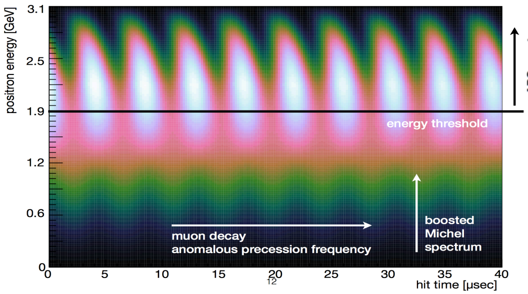


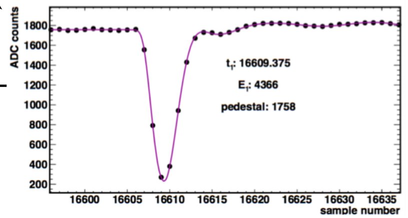


Calibrates and reconstructs the energy.

**Total Systematic Uncertainty**

**BNL to FNAL**

**180 ppb to 70 ppb**

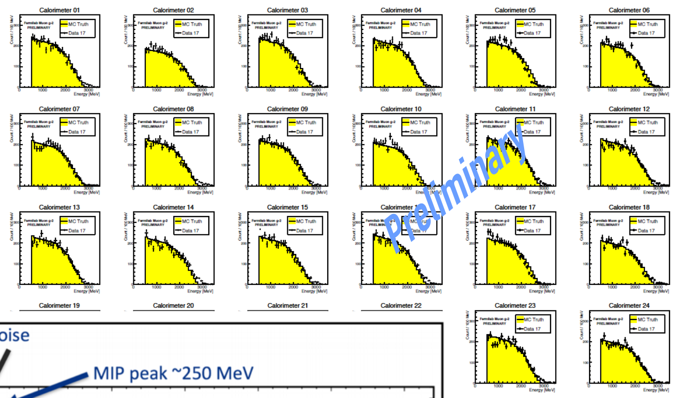


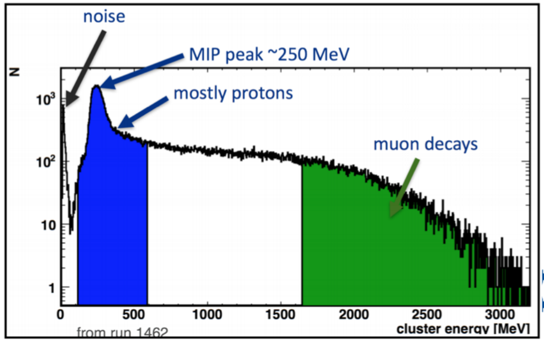


Fit the time spectrum of the acceptance and resolution corrected energy distribution.

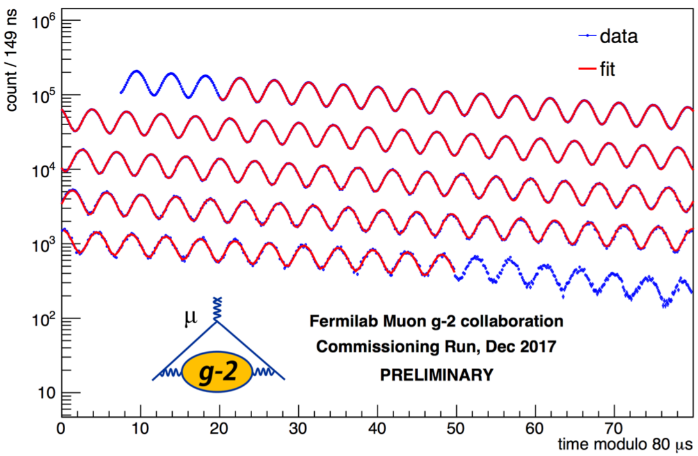




Fermilab

$$a_\mu(\mathrm{Expt}) = \frac{g_e}{2}\frac{\omega_a}{\tilde{\omega}_p}\frac{m_\mu}{m_e}\frac{\mu_p}{\mu_e}$$

$$a_\mu(\mathrm{Expt}) \approx \frac{\omega_a}{\omega_p \otimes \rho(r)}$$

To measure the magnetic field as seen by the muons ( $\tilde{\omega}_p$ ), we need to measure the spatial distribution of the muon beam.

Corrections are applied to $\omega_a$ , those corrections are related to the dynamics of the beam.

$$a_\mu(\mathrm{Expt}) \approx \frac{\omega_a}{\omega_p \otimes \rho(r)}$$

B-field = 1.45 T

Tracking detectors measure the muon beam.

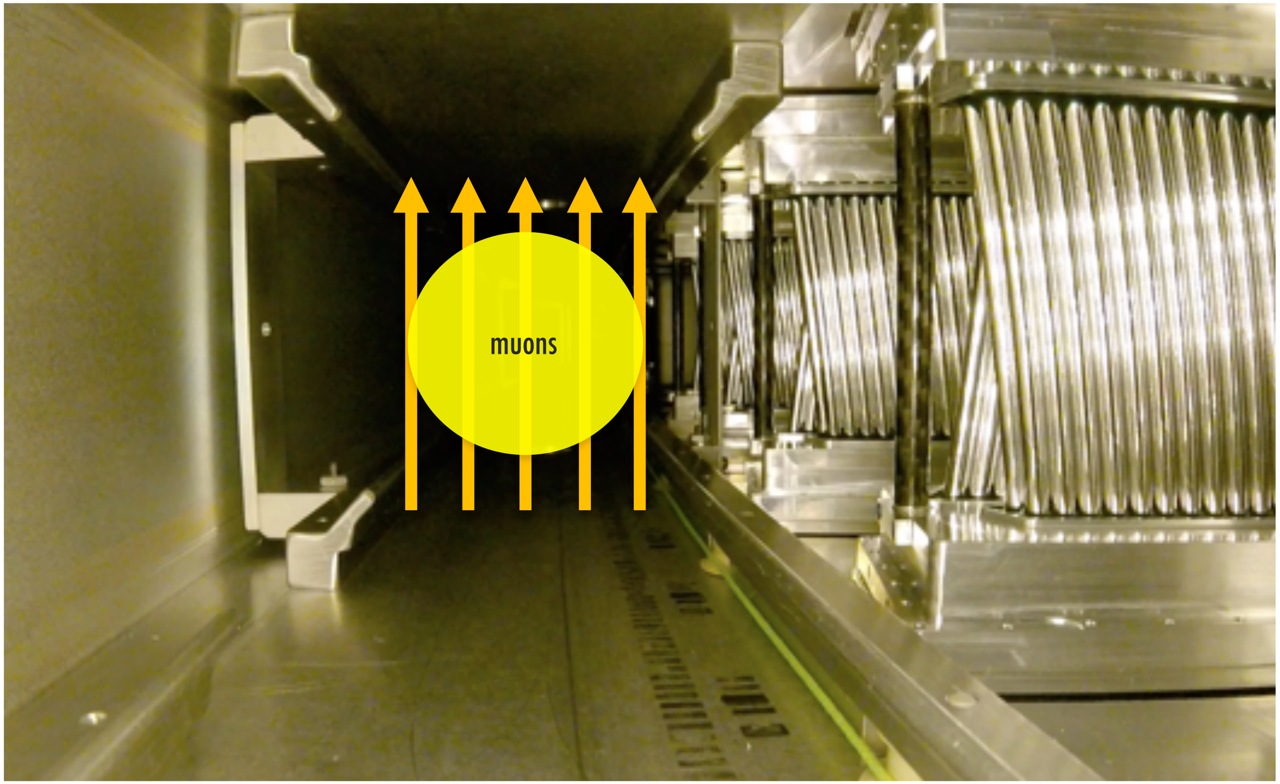

$$a_\mu(\text{Expt}) \approx \frac{\omega_a}{\omega_p \otimes \rho(r)}$$

B-field = 1.45 T

Tracking detectors measure the muon beam.

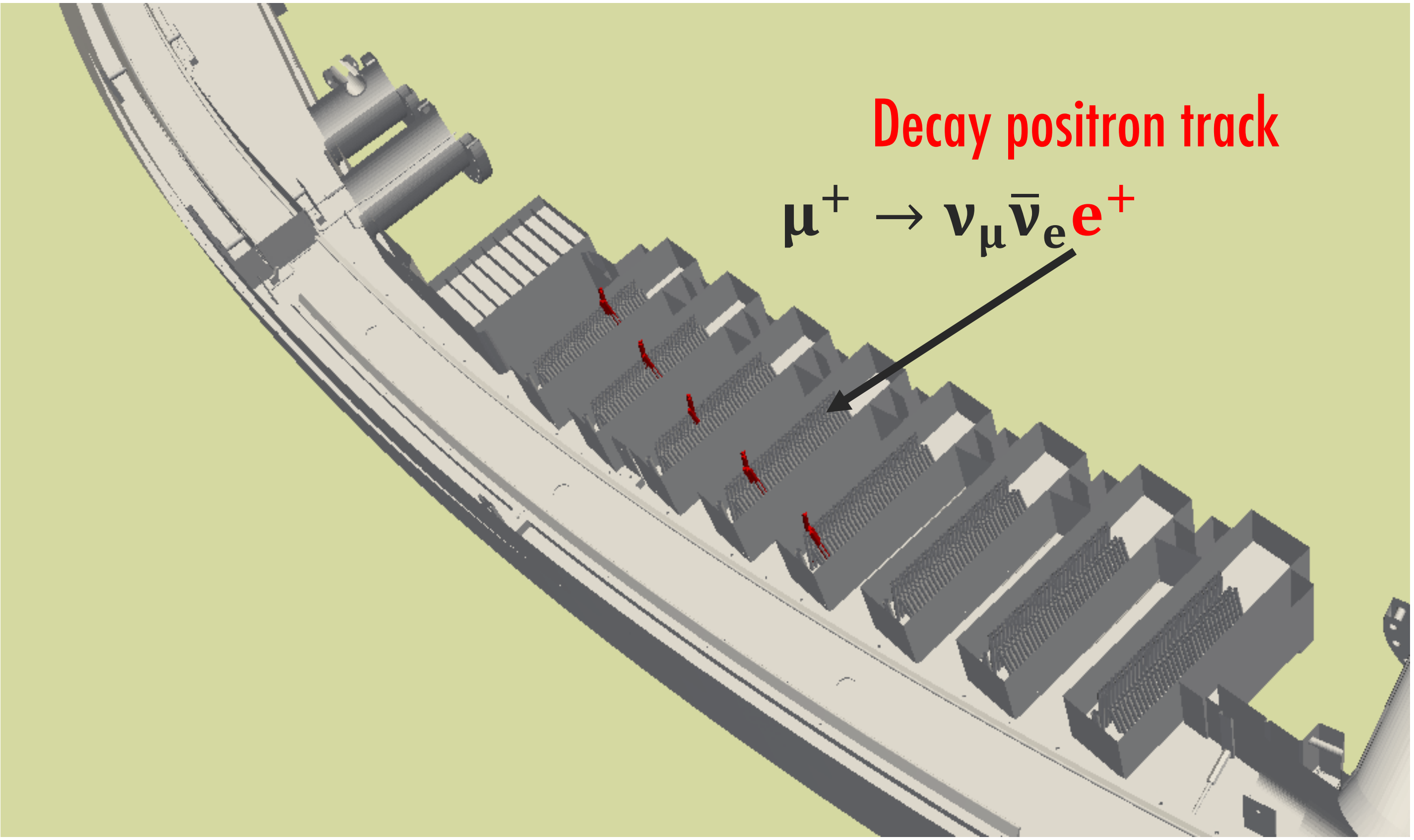

$$a_\mu(\text{Expt}) \approx \frac{\omega_a}{\omega_p \otimes \rho(r)}$$

B-field = 1.45 T

Tracking detectors measure the muon beam.

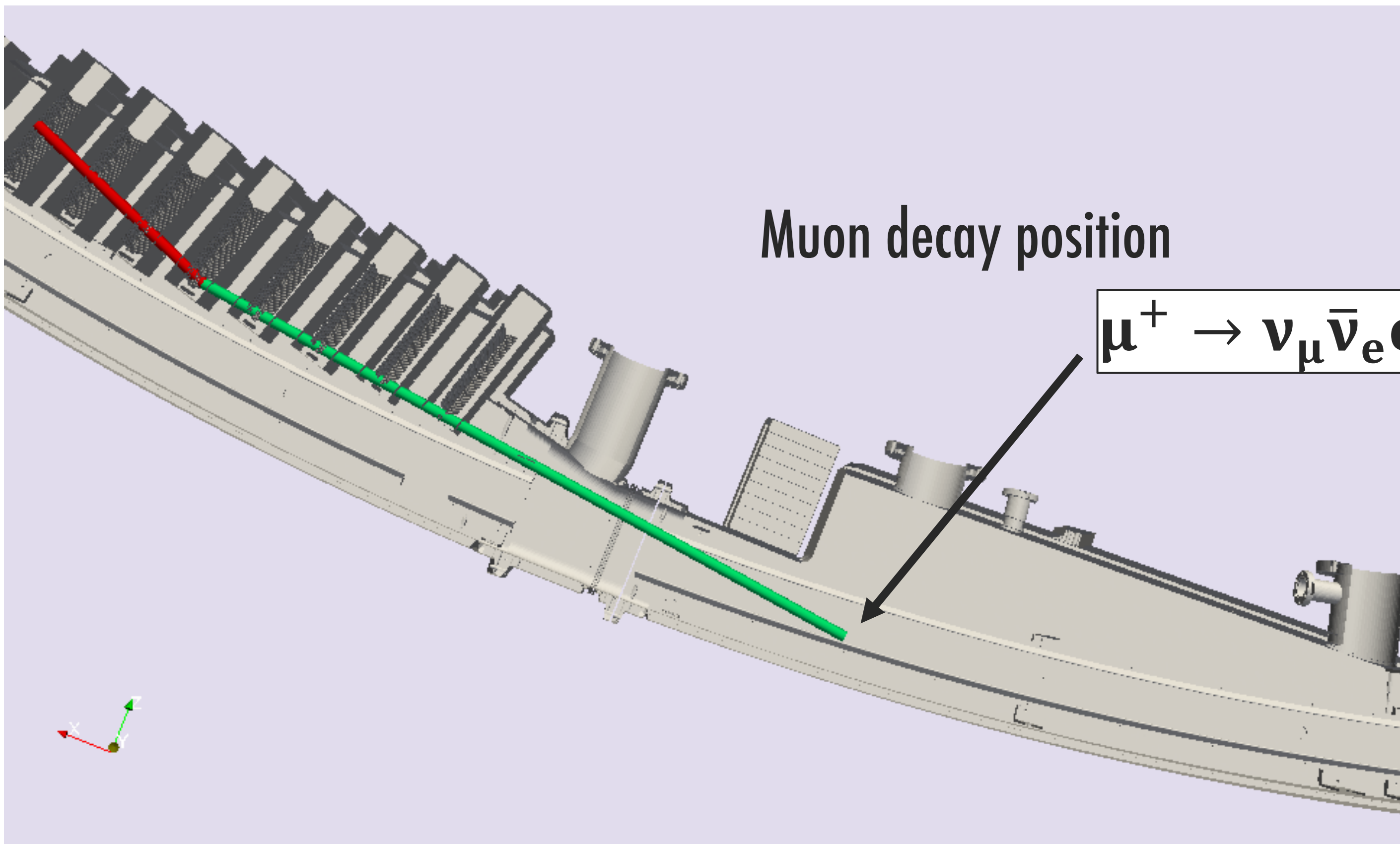


$$\mu^+ \rightarrow \nu_\mu \bar{\nu}_e e^+$$

$$a_\mu(\mathrm{Expt}) \approx \frac{\omega_a}{\omega_p \otimes \rho(r)}$$

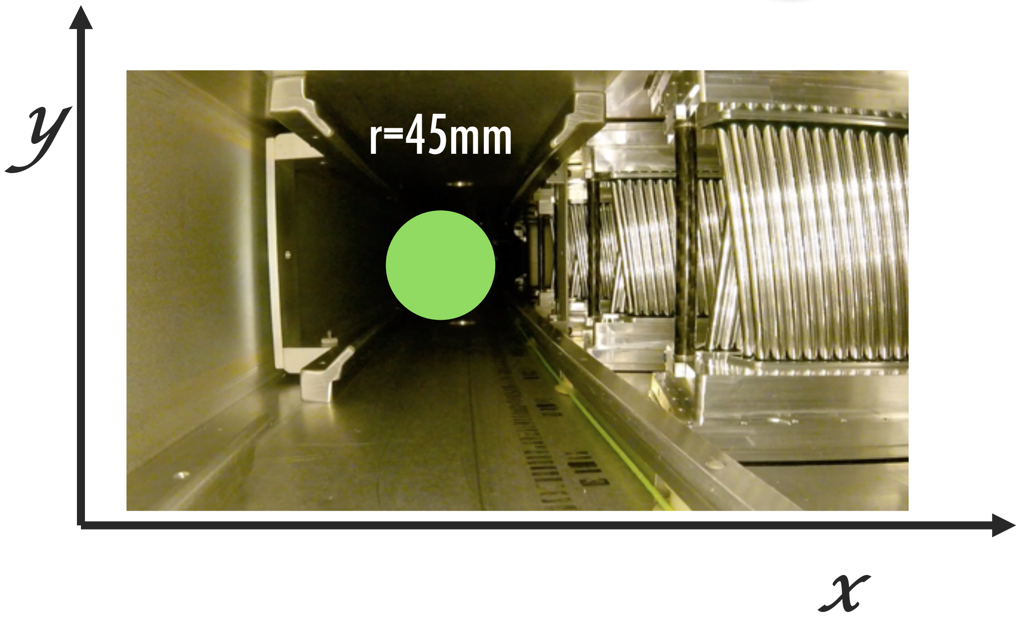


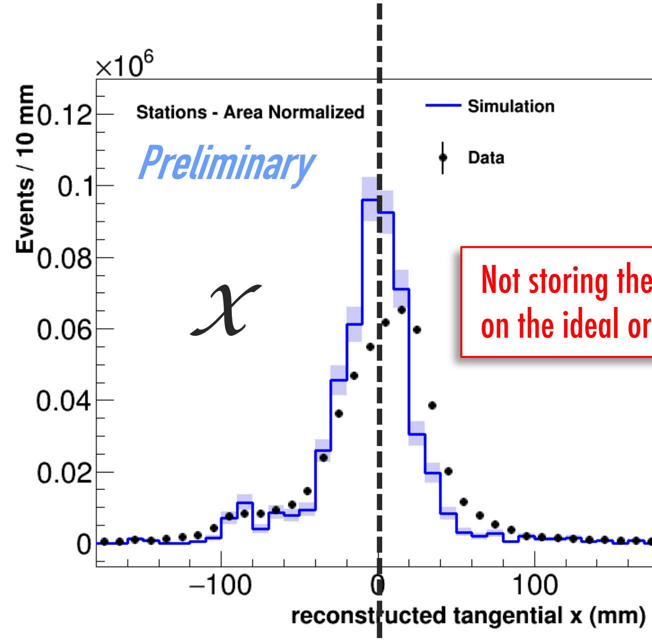


Not storing the beam on the ideal orbit!

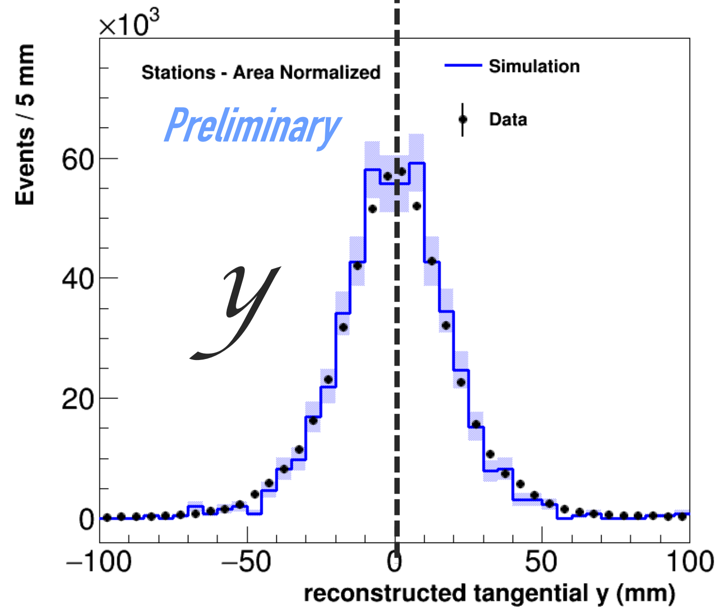

As you know, there are always new challenges when an experiment begins the physics run!

Detangling the dynamics of the beam : Investigating a possible problem

Inflector magnet safely guides the beam into muon storage ring.

The beam enters the muon storage ring at a displaced position from the ideal orbit.

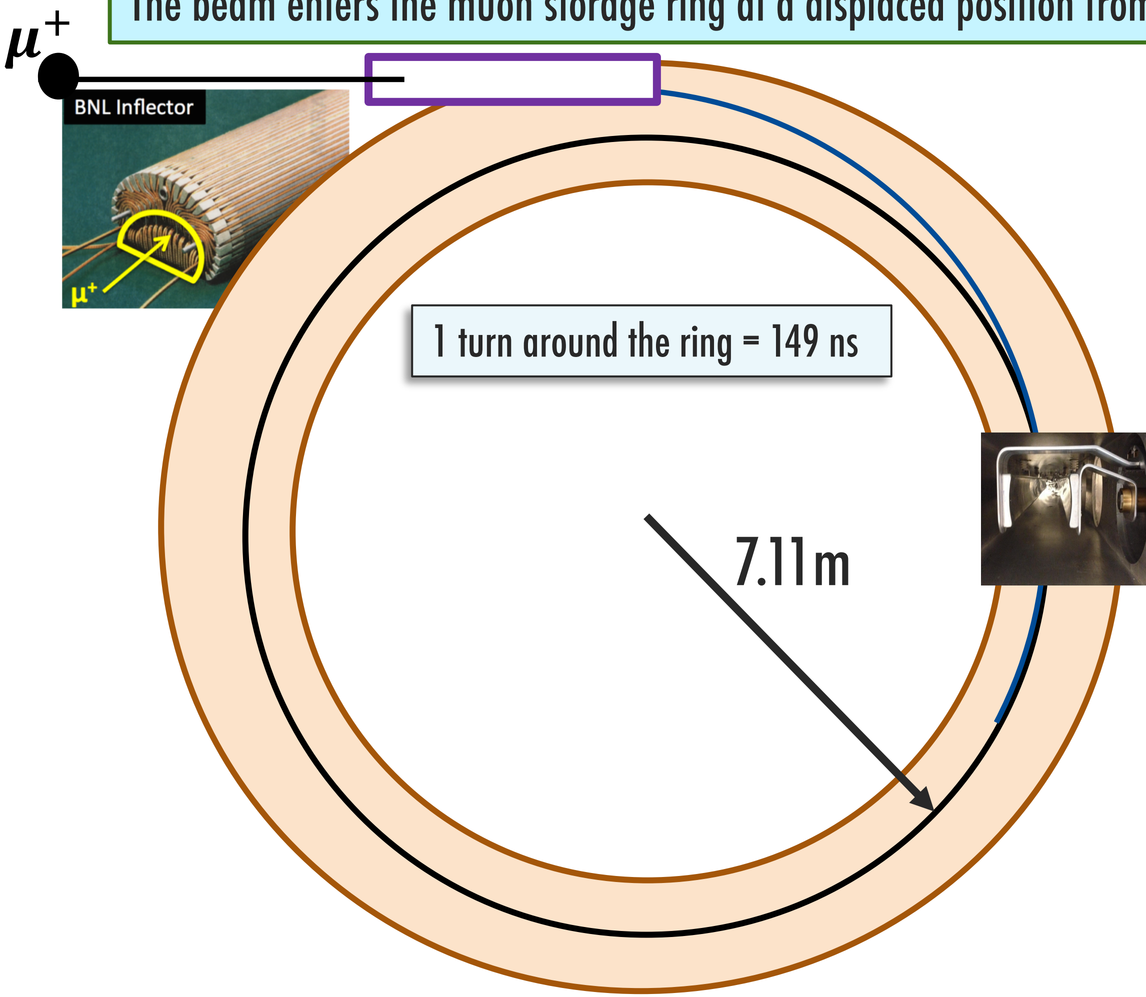


Blumlein Kicker Magnet kicks the beam onto the storage ring ideal orbit.

# The inflector magnet and the muon storage ring have different beam phase space distributions!

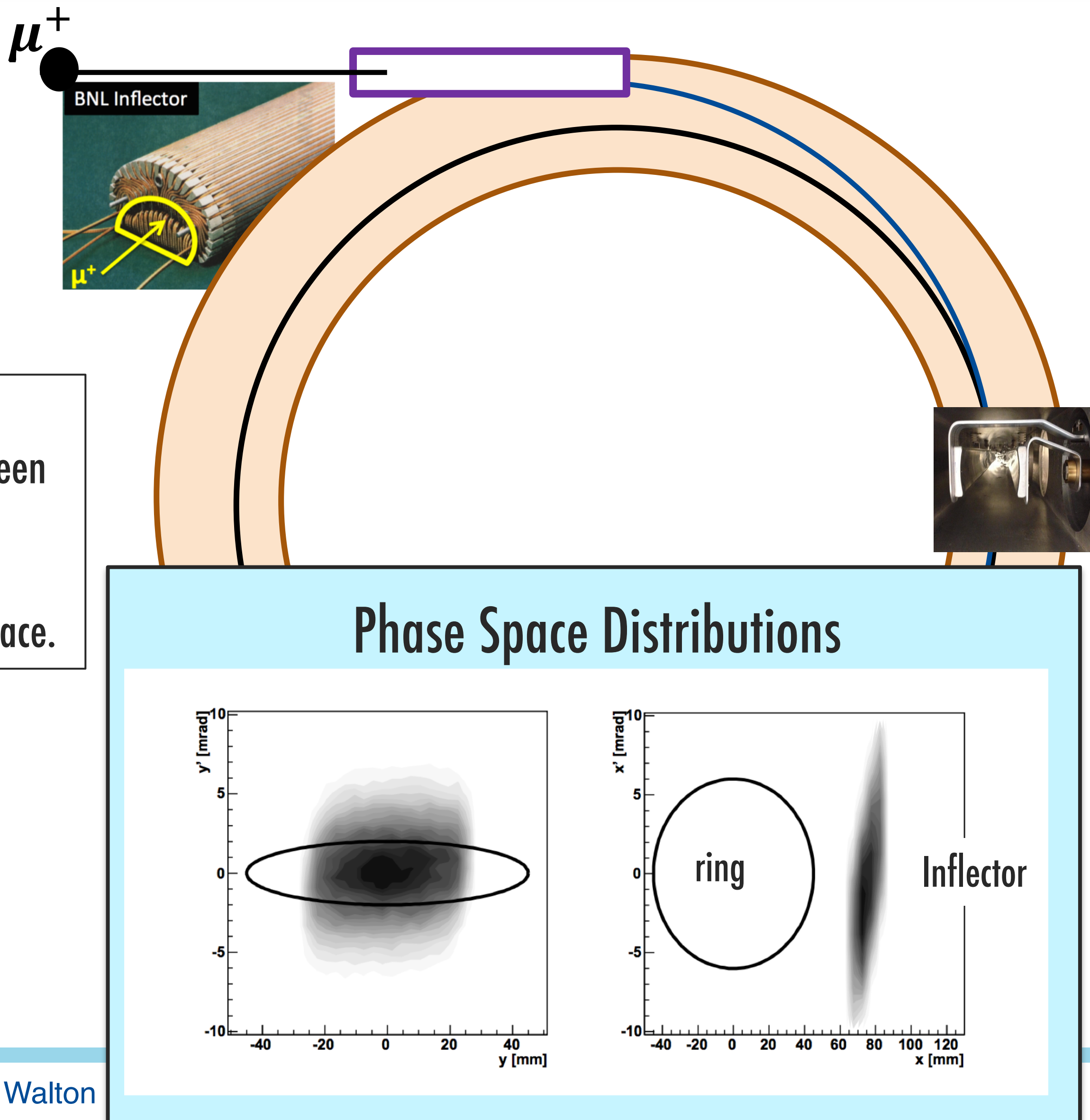


Insensitive to differences between the infector and storage ring in vertical phase space.

Due to the efficiency and acceptance of the kick, the beam is sensitive to differences between the infector and storage ring in radial phase space.

Creates coherent betatron oscillations in the radial direction!



Fermilab

# Radial Coherent Betatron Oscillations (CBO):

- Mismatch between inflector and ring phase space
- Under kicking the beam on the storage ring orbit

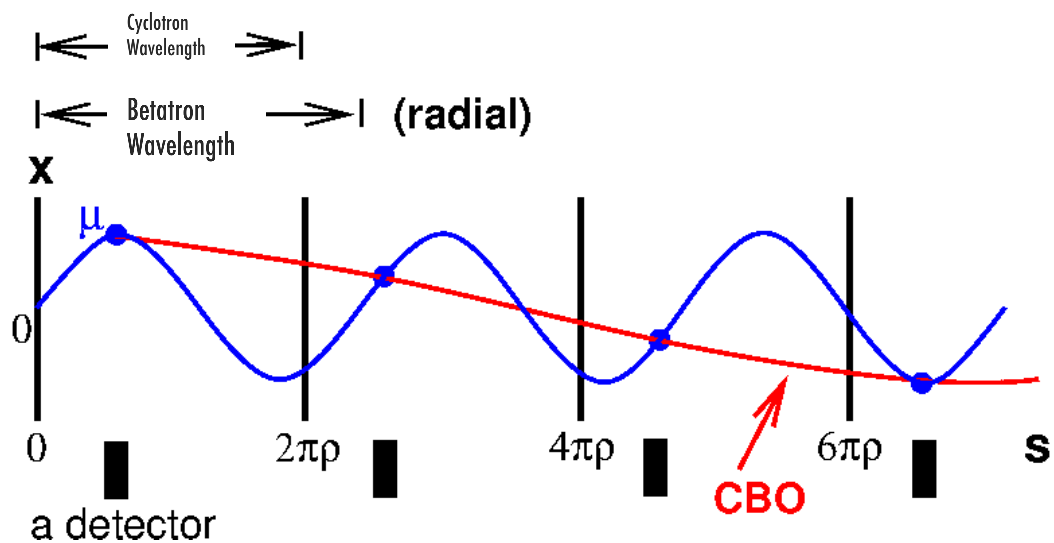


For the Brookhaven Muon g-2 experiment (PREVIOUS EXPERIMENT) :

- The CBO wavelength = 14.1 × 149 ns
- The CBO lifetime is about 100 – 140 microseconds

The CBO is an unwanted signal!! It is problematic because the CBO affects the detector acceptance and extraction of the spin precession frequency if $\omega_{CBO} = N\omega_a$ : $(\omega_a = 4.37\ \mu s)$ .

# Measuring the Radial Coherent Betatron Oscillations

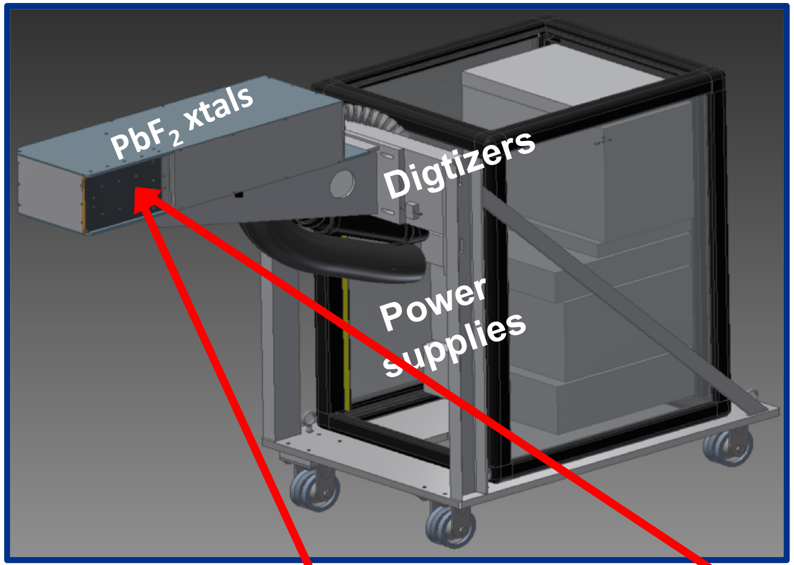


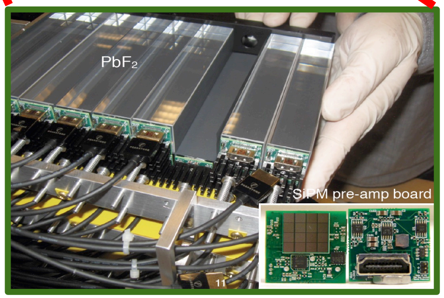


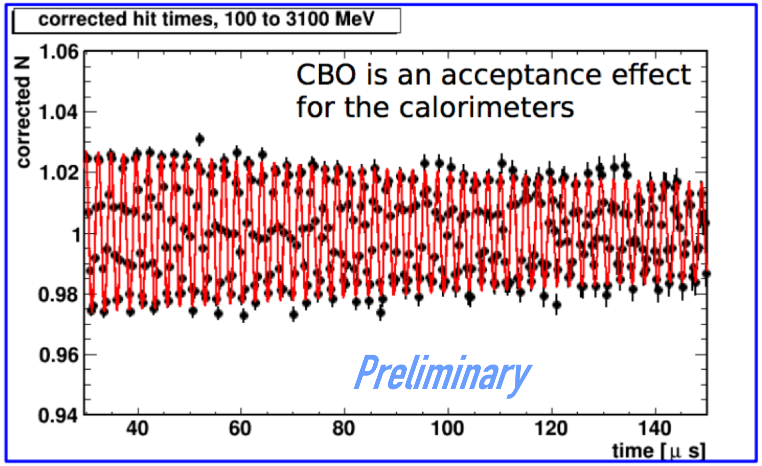


Results using the calorimeters

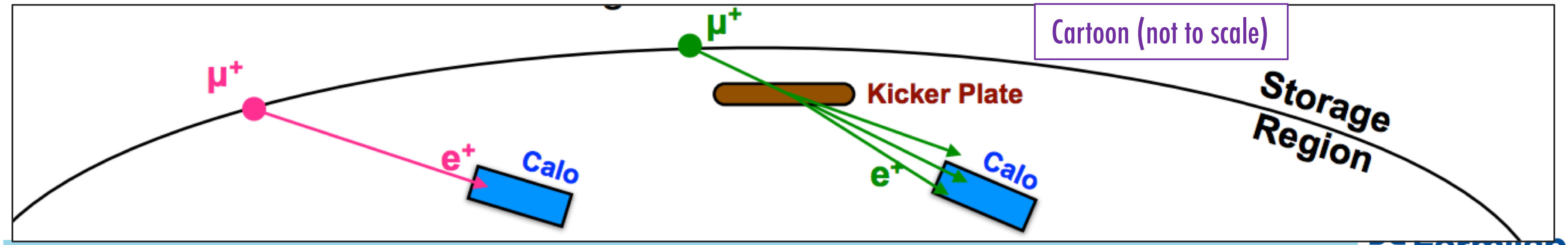

# Measuring the Radial Coherent Betatron Oscillations

$f_{CBO} = 2.10\ \mu s$

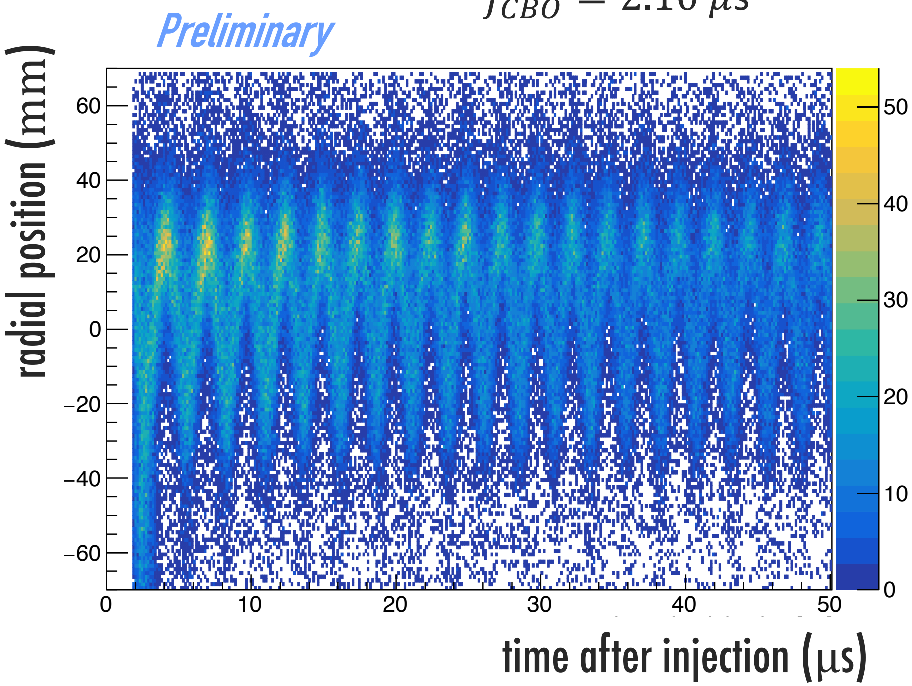


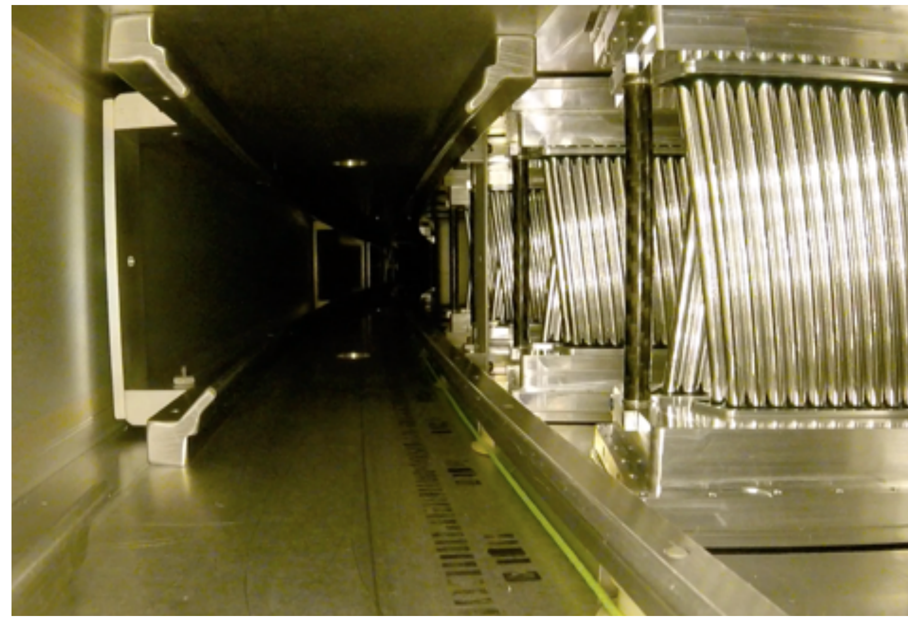

Results using the tracking detectors

# Measuring the Radial Coherent Betatron Oscillations

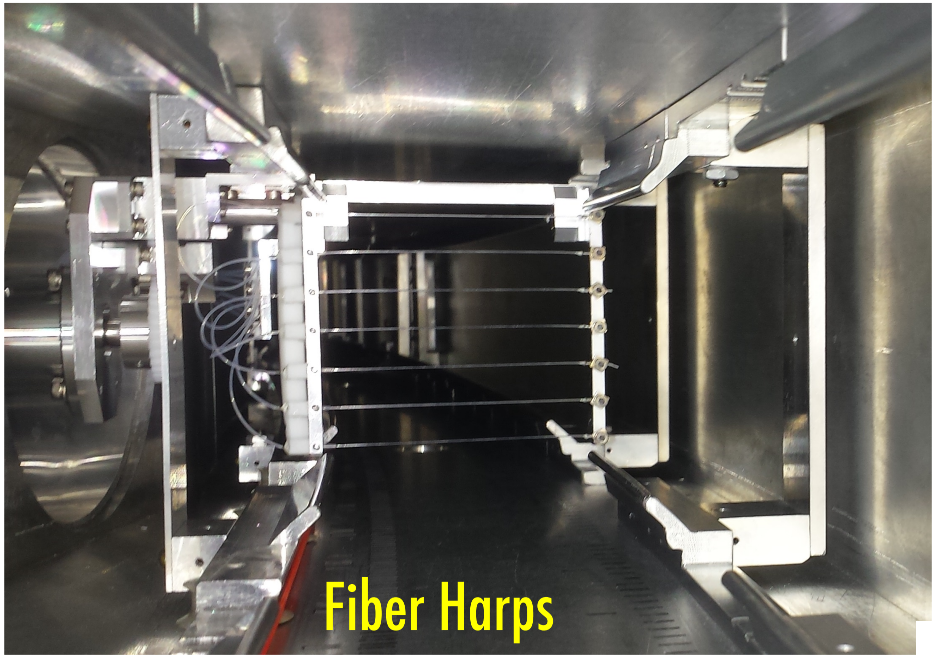


Results using the destructive detectors in the muon storage ring.

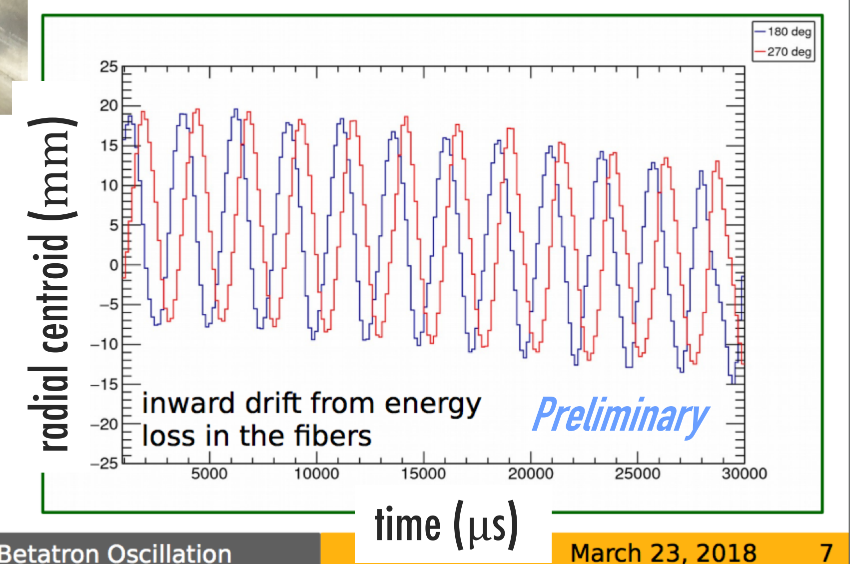

# Measuring the Radial Coherent Betatron Oscillations

## CBO amplitude and life-time

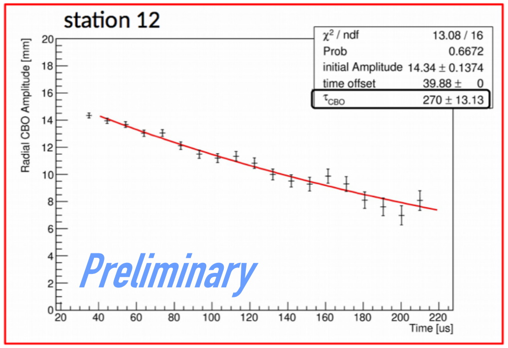


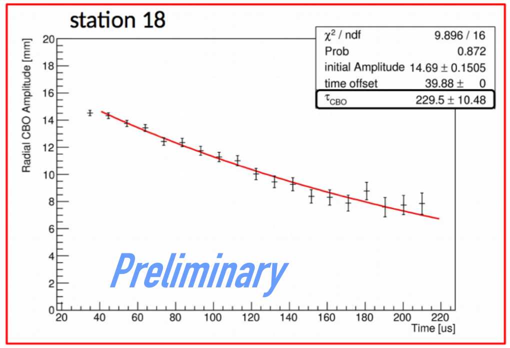


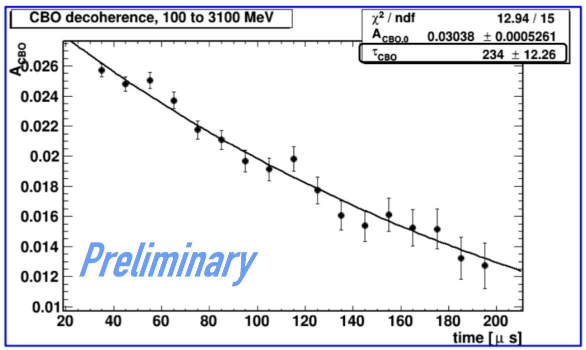


CBO life-time (55 kV kick):
~245 μs (Trackers+Calorimeters)

CBO amplitude (55 kV kick):
~14.5 mm at 35 μs (Trackers)
~13 mm at 1 μs (Fiber Harps)
~2.6%[1] at 30 μs (Calorimeters)

Antoine *et al.* Coherent Betatron Osci

While commissioning the experiment, the FNAL detectors are seeing a much larger CBO amplitude and longer lifetime compared with the final measurements from BNL.

For the Brookhaven Muon g-2 experiment, the CBO :

- lifetime is about $100 - 140\ \mu s$

CBO Systematic Uncertainty
BNL to FNAL
70 ppb to >30 ppb

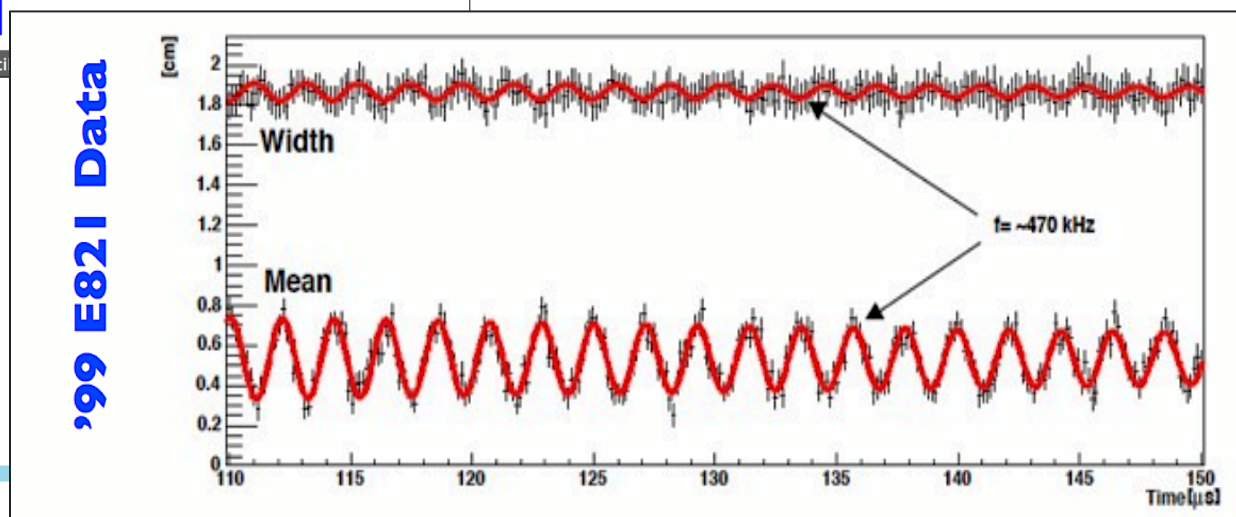

Inflector magnet safely guides the beam into muon storage ring.

The beam enters the muon storage ring at a displaced position from the ideal orbit.

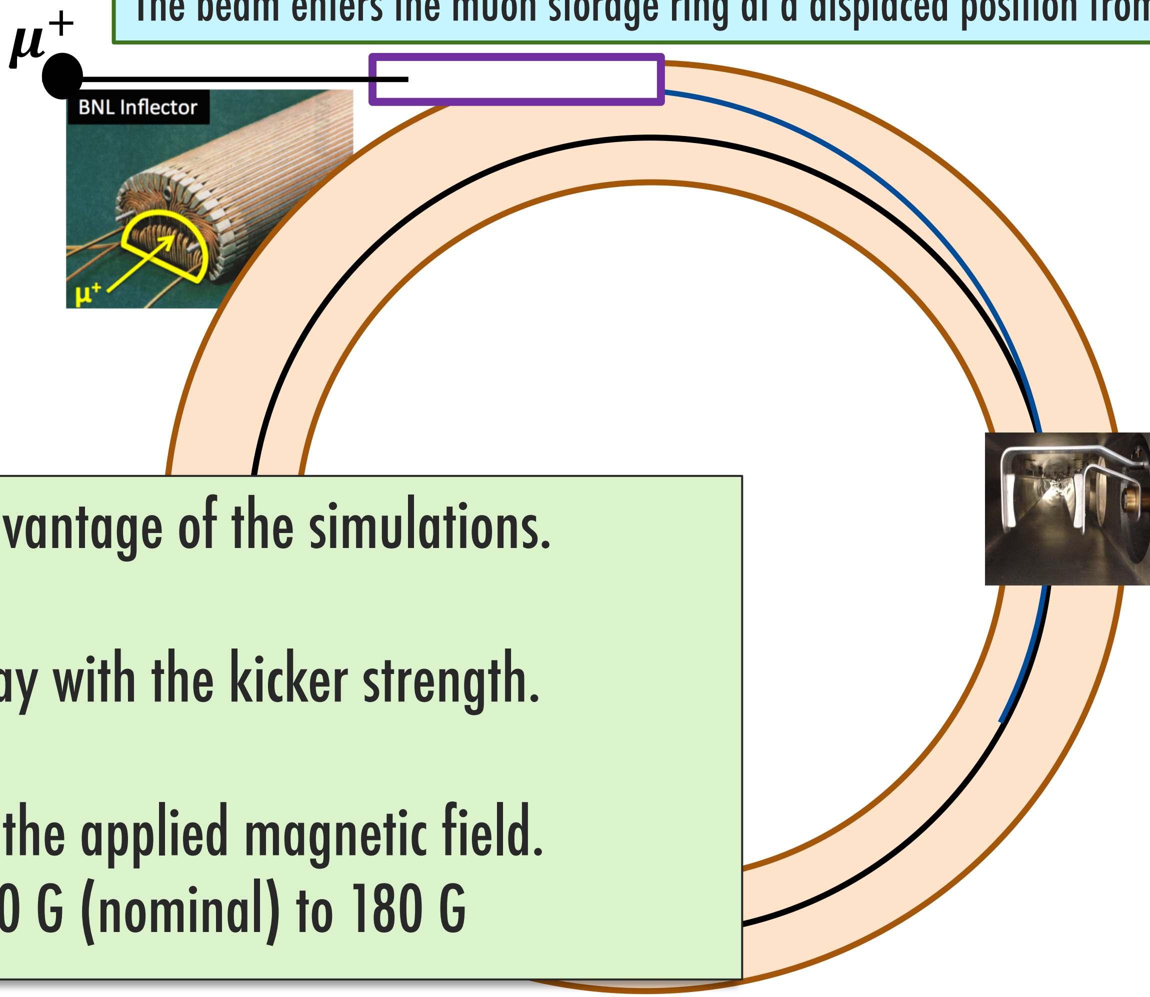


Blumlein Kicker Magnet kicks the beam onto the storage ring ideal orbit.

- Take advantage of the simulations.
- Let’s play with the kicker strength.
- Reduce the applied magnetic field.
    - 260 G (nominal) to 180 G

$$a_\mu(\mathrm{Expt}) \approx \frac{\omega_a}{\omega_p \;\otimes\; \rho(r)}$$

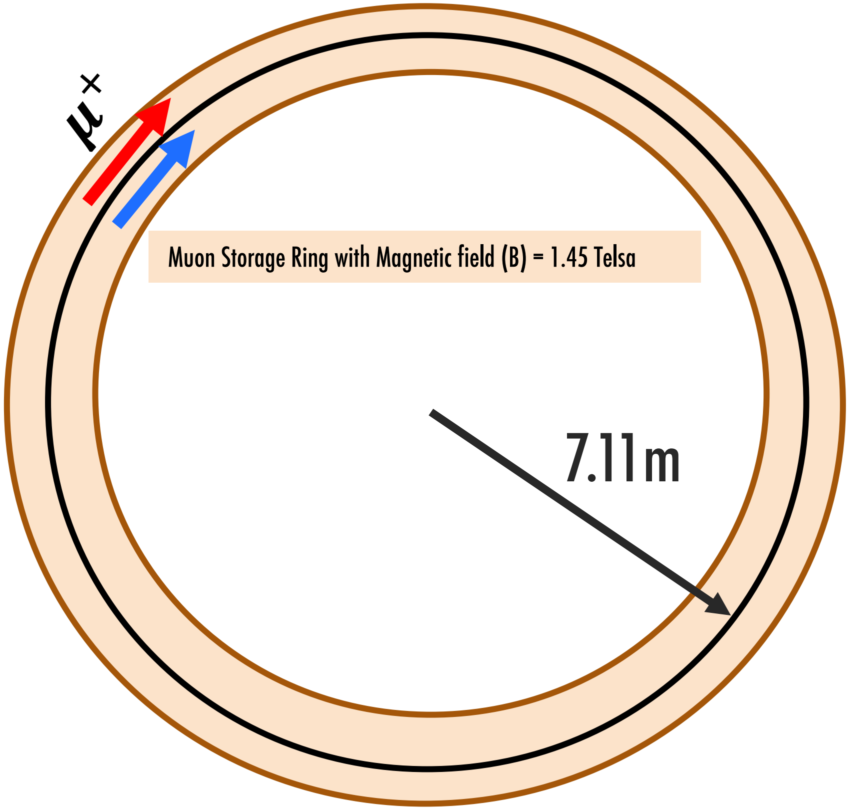


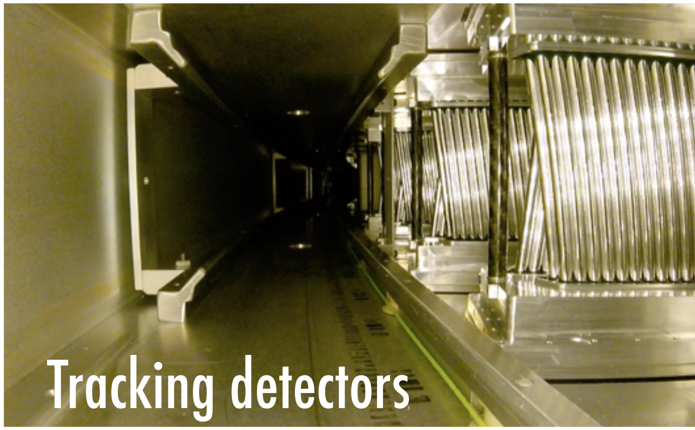


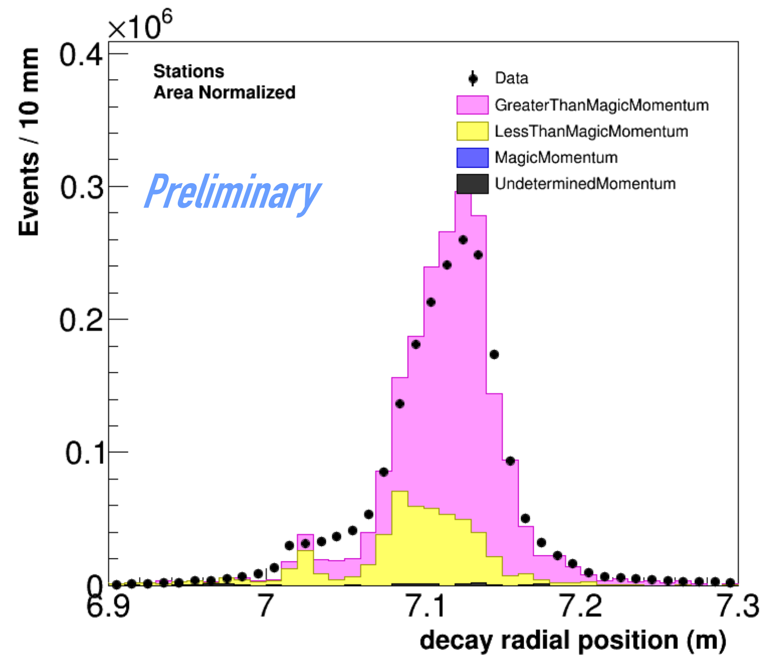


- An inefficient kick is part of the problem.
- To determine if it is the only and primary source, we still need to run additional tests and studies.

# Outline

- Muon g-2 Physics
- Muon g-2 Experiment
- Muon g-2 Status
- Conclusions

- Muon g-2 experiment is operational, running, and taking physics data.
- The experiment is working hard to understand the dynamics of the beam.
- Unlike the Brookhaven Muon g-2 experiment, there are highly developed tracking detectors and simulation tools which will help us quickly solve the problems and control the systematic uncertainties.
- Look forward to the first results of $a_\mu$ from Fermilab Muon g-2 experiment.

# 8 Countries, 35 Institutions, 190 Collaborators


# Back-up Slides

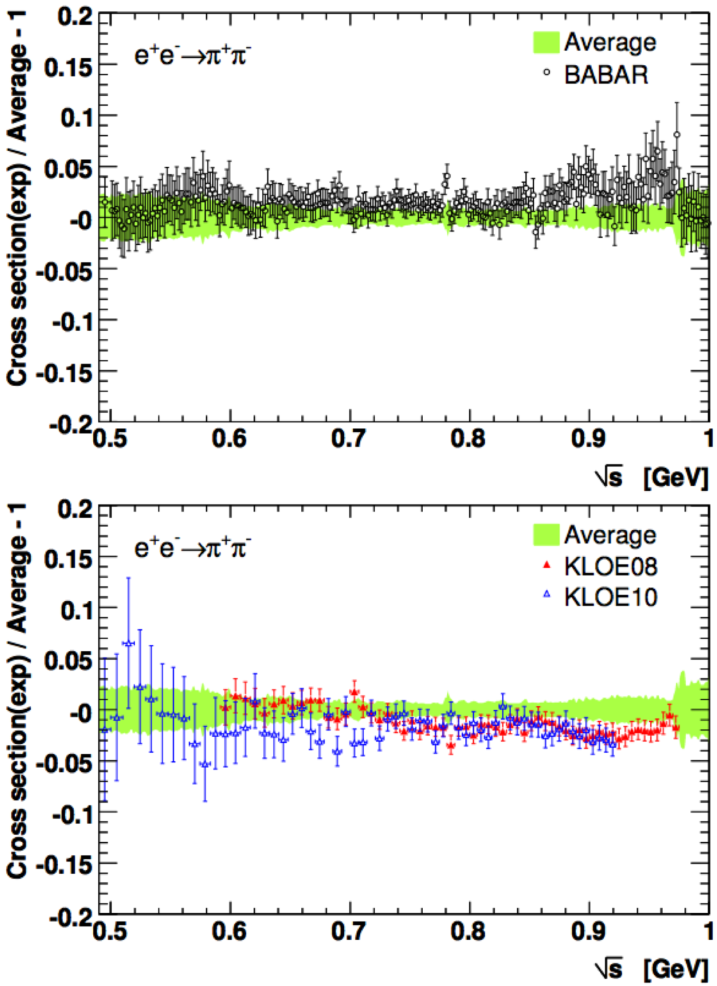


Figure 3: Comparison between individual $e^+e^- \to \pi^+\pi^-$ cross section measurements from BABAR (top) and KLOE (bottom) and the HVPTools average.

https://arxiv.org/pdf/1302.1896.pdf

| | $\delta(\sigma)/\sigma$ present | $\delta a_\mu$present | $\delta(\sigma)/\sigma$ future | $\delta a_\mu$future |
|---|---|---|---|---|
| $\sqrt{s} < 1$ GeV | 0.7% | 33 | 0.4% | 19 |
| $1 < \sqrt{s} < 2$ GeV | 6% | 39 | 2% | 13 |
| $\sqrt{s} > 2$ GeV | | 12 | | 12 |
| total | | 53 | | 26 |

Table 2.4: Overall uncertainty of the cross-section measurement required to get the reduction of uncertainty on $a_\mu$ in units $10^{-11}$ for three regions of $\sqrt{s}$ (from Ref. [93]).

The deviations for particular energy range between BABAR and KLOE make it difficult for performing various data combinations.

https://arxiv.org/pdf/1710.06874.pdf

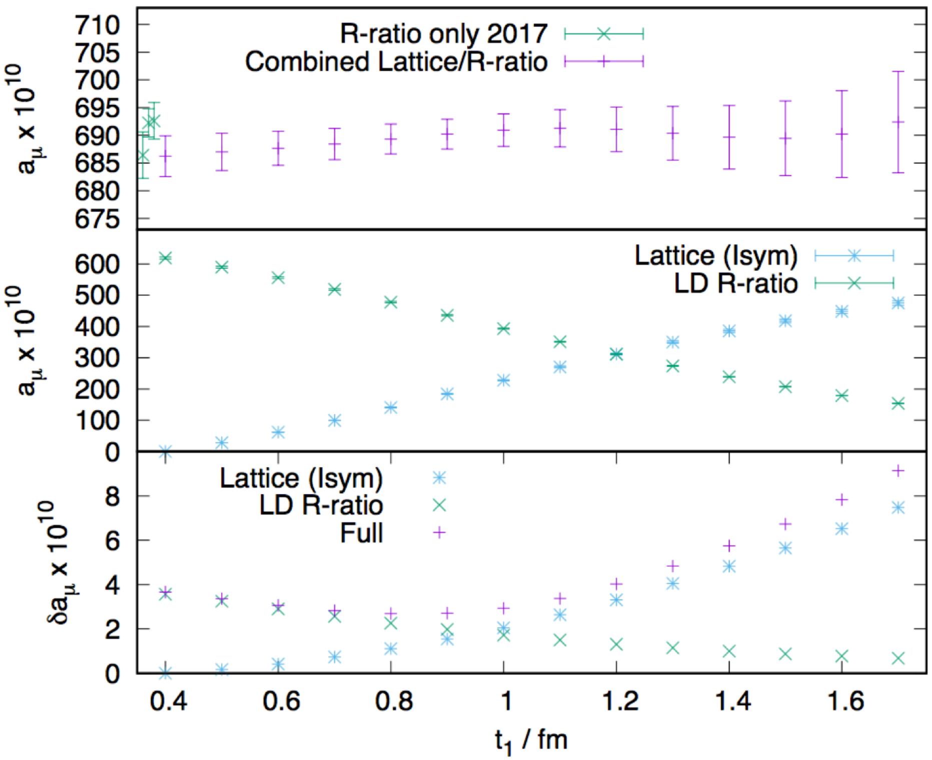

$$a_\mu(\mathrm{SUSY}) \cong \left(\mathrm{sgn}(\mu)\, 130\times10^{-11} \tan\beta \left({}^{100\mathrm{GeV}}/_{\tilde{m}}\right)^2\right)$$

$$a_\mu^{\mathrm{EXP}} - a_\mu^{\mathrm{SM}} = a_\mu^{\mathrm{New\ Physics}}$$

D. Hertzog, Ann. Phys (Berlin) 2015., courtesy D. Stockinger

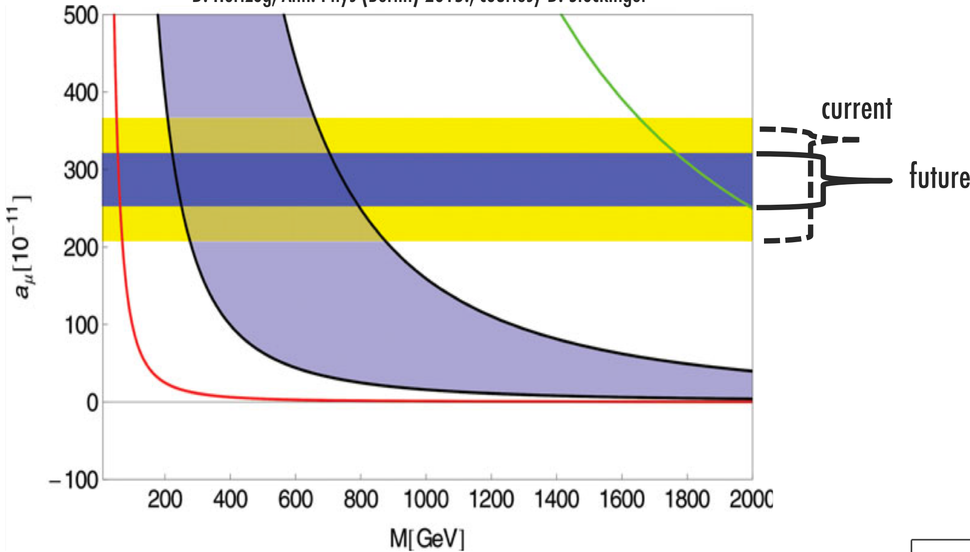


- Z′, W′, UED, Littlest Higgs (assumes typical weak coupling) $\mathcal{O}\left(\frac{\alpha}{4\pi}\right)$
- Radiative muon mass generation $\mathcal{O}\,(\,1)$ in supersymmetry
- Extra Dimension Models, SUSY ($\tan\beta$ = 5 to 50) $\mathcal{O}\left(\frac{\alpha}{4\pi}..\right)$

$a_\mu(\mathrm{SUSY})$ contributions arise from sleptons and charginos and LHC is sensitive to squarks and gluinos.

Results from Muon g-2 experiment will be complementary to the physics at the Large Hadron Collider (LHC).

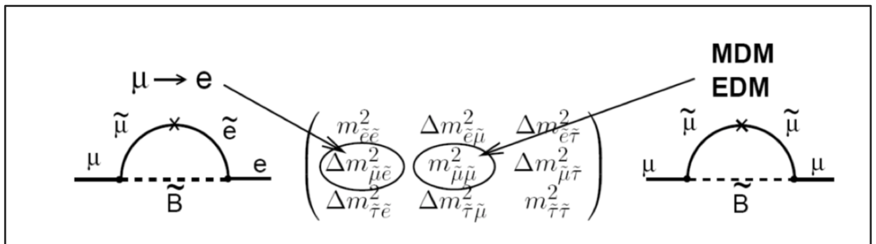


$$\delta a_\mu^{\mathrm{New\ Physics}} = \mathcal{O}(1) \times \left(\frac{m_\mu}{\Lambda}\right)^2 \times \left(\frac{\delta m_\mu^{New\ Physics}}{m_\mu}\right)$$

| Names | Spin | $P_R$ | Gauge Eigenstates | Mass Eigenstates |
|---|---|---|---|---|
| Higgs bosons | 0 | +1 | $H_u^0\ H_d^0\ H_u^+\ H_d^-$ | $h^0\ H^0\ A^0\ H^\pm$ |
| squarks | 0 | −1 | $\tilde{u}_L\ \tilde{u}_R\ \tilde{d}_L\ \tilde{d}_R$<br>$\tilde{s}_L\ \tilde{s}_R\ \tilde{c}_L\ \tilde{c}_R$<br>$\tilde{t}_L\ \tilde{t}_R\ \tilde{b}_L\ \tilde{b}_R$ | (same)<br>(same)<br>$\tilde{t}_1\ \tilde{t}_2\ \tilde{b}_1\ \tilde{b}_2$ |
| sleptons | 0 | −1 | $\tilde{e}_L\ \tilde{e}_R\ \tilde{\nu}_e$<br>$\tilde{\mu}_L\ \tilde{\mu}_R\ \tilde{\nu}_\mu$<br>$\tilde{\tau}_L\ \tilde{\tau}_R\ \tilde{\nu}_\tau$ | (same)<br>(same)<br>$\tilde{\tau}_1\ \tilde{\tau}_2\ \tilde{\nu}_\tau$ |
| neutralinos | 1/2 | −1 | $\tilde{B}^0\ \tilde{W}^0\ \tilde{H}_u^0\ \tilde{H}_d^0$ | $\tilde{N}_1\ \tilde{N}_2\ \tilde{N}_3\ \tilde{N}_4$ |
| charginos | 1/2 | −1 | $\tilde{W}^\pm\ \tilde{H}_u^+\ \tilde{H}_d^-$ | $\tilde{C}_1^\pm\ \tilde{C}_2^\pm$ |
| gluino | 1/2 | −1 | $\tilde{g}$ | (same) |
| goldstino (gravitino) | 1/2 (3/2) | −1 | $\tilde{G}$ | (same) |

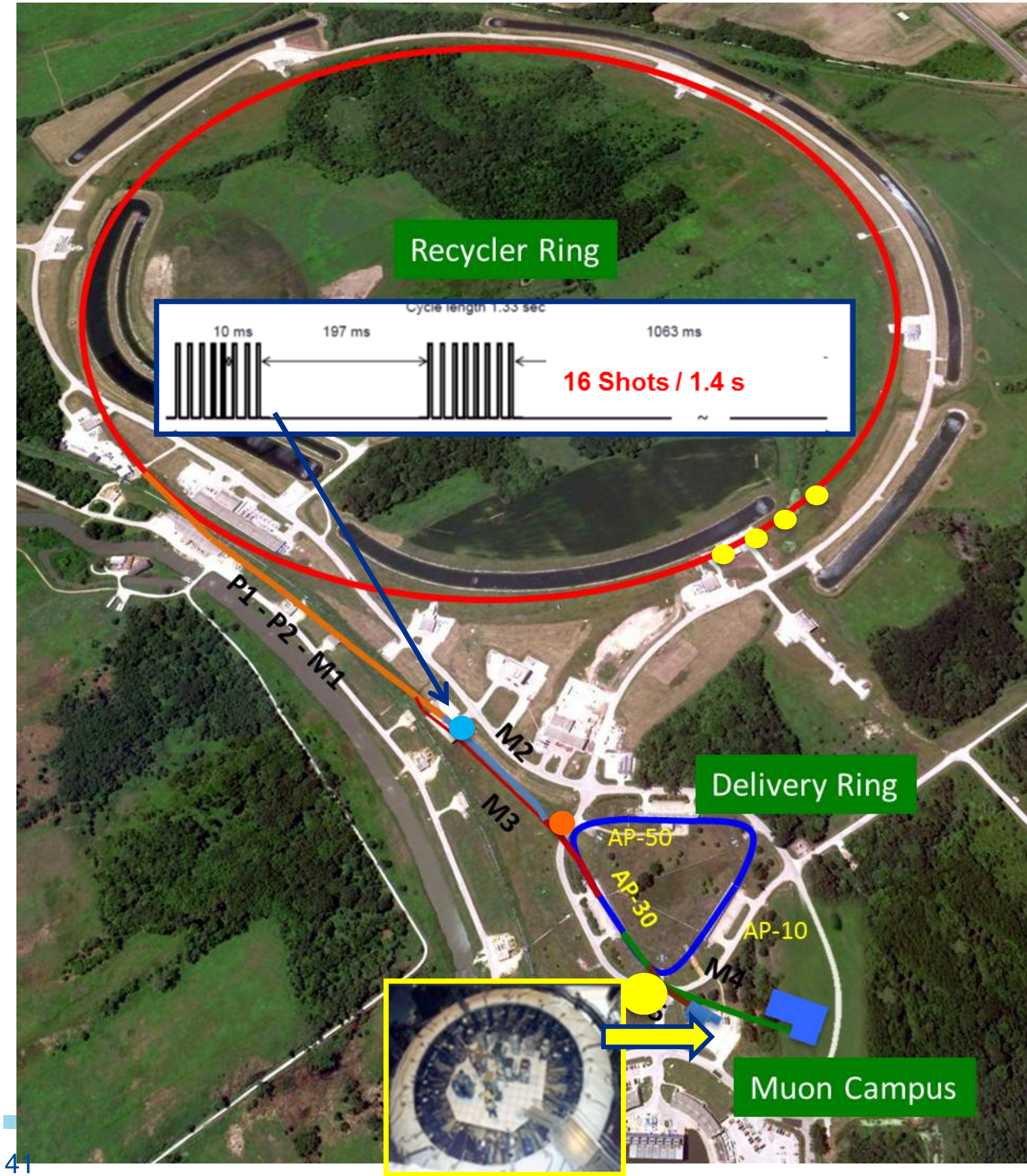


Delivers $10^{12}$ 8-GeV proton batches to the Main Injector Recycler.

Batches are split into four bunches.

Each bunch collides with a fixed target.

3.1 GeV pions are selected and focused to the delivery ring.

Pion decay into muon while turning around the delivery ring.

Muons are focused and injected into the Muon g-2 storage ring.

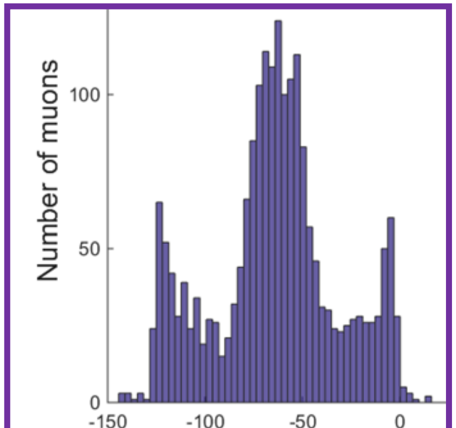


Intensity profile is 120 ns wide with "W" shape ( Model )

Since the beam is non-monoenergetic, the beam motion in the electric field contributes to the frequency.

$$\boxed{\omega_a = \frac{q}{m_\mu c}\left[a_\mu B - \left(a_\mu - \frac{1}{\gamma^2 - 1}\right)(\beta \times E)\right]}$$

The injected beam has a vertical motion and the electromagnetic restoring force induces a magnetic motion.

$$\boxed{\omega_a = \frac{q}{m_\mu c}\left[a_\mu B - a_\mu\left(\frac{\gamma}{\gamma + 1}\right)(\beta \cdot B)\beta - \left(a_\mu - \frac{1}{\gamma^2 - 1}\right)(\beta \times E)\right]}$$

For $\boxed{\gamma = 29.3 \rightarrow p_\mu = 3.09\ \mathrm{GeV/c}}$

The coefficient vanishes and giving the magic momentum of 3.09 GeV/c!
To satisfy the magic momentum condition, the orbit radius is 7.112 meters.
Assume the beam is moving perpendicular to the magnetic field.

$$\boxed{\omega_a = \frac{q}{m_\mu c}\left[a_\mu B - \cancel{a_\mu\left(\frac{\gamma}{\gamma + 1}\right)(\beta \cdot B)\beta} - \cancel{\left(a_\mu - \frac{1}{\gamma^2 - 1}\right)}(\beta \times E)\right]}$$

$$a_\mu(\text{Expt}) = \frac{g_e}{2}\frac{\omega_a}{\tilde{\omega}_p}\frac{m_\mu}{m_e}\frac{\mu_p}{\mu_e}$$

## Systematic Sources for $\tilde{\omega}_p$

| Category | E821 [ppb] | Main E989 Improvement Plans | Goal [ppb] |
|---|---|---|---|
| Absolute field calibration | 50 | Special 1.45 T calibration magnet with thermal enclosure; additional probes; better electronics | 35 |
| Trolley probe calibrations | 90 | Plunging probes that can cross calibrate off-central probes; better position accuracy by physical stops and/or optical survey; more frequent calibrations | 30 |
| Trolley measurements of $B_0$ | 50 | Reduced position uncertainty by factor of 2; improved rail irregularities; stabilized magnet field during measurements* | 30 |
| Fixed probe interpolation | 70 | Better temperature stability of the magnet; more frequent trolley runs | 30 |
| Muon distribution | 30 | Additional probes at larger radii; improved field uniformity; improved muon tracking | 10 |
| Time-dependent external magnetic fields | – | Direct measurement of external fields; simulations of impact; active feedback | 5 |
| Others † | 100 | Improved trolley power supply; trolley probes extended to larger radii; reduced temperature effects on trolley; measure kicker field transients | 30 |
| Total systematic error on $\omega_p$ | 170 | | 70 |

## Systematic Sources for $\omega_a$

| Category | E821 [ppb] | E989 Improvement Plans | Goal [ppb] |
|---|---|---|---|
| Gain changes | 120 | Better laser calibration | |
| | | low-energy threshold | 20 |
| Pileup | 80 | Low-energy samples recorded | |
| | | calorimeter segmentation | 40 |
| Lost muons | 90 | Better collimation in ring | 20 |
| CBO | 70 | Higher $n$ value (frequency) | |
| | | Better match of beamline to ring | $< 30$ |
| $E$ and pitch | 50 | Improved tracker | |
| | | Precise storage ring simulations | 30 |
| Total | 180 | Quadrature sum | 70 |



Fermilab

Table 4.1: Frequencies in the $(g-2)$ storage ring, assuming that the quadrupole field is uniform in azimuth and that $n = 0.137$.

| Quantity | Expression | Frequency [MHz] | Period [$\mu$s] |
|---|---|---|---|
| $f_a$ | $\frac{e}{2\pi mc} a_\mu B$ | 0.228 | 4.37 |
| $f_C$ | $\frac{v}{\pi R_0}$ | 6.7 | 0.149 |
| $f_x$ | $\sqrt{1-n} f_c$ | 6.23 | 0.160 |
| $f_y$ | $\sqrt{n} f_c$ | 2.48 | 0.402 |
| $f_{\mathrm{CBO}}$ | $f_c - f_x$ | 0.477 | 2.10 |
| $f_{\mathrm{VW}}$ | $f_c - 2f_y$ | 1.74 | 0.574 |

$$a_\mu(\text{Expt}) \approx \frac{\omega_a}{\omega_p \otimes \rho(r)}$$